RECOGDRIVE: A REINFORCED COGNITIVE FRAMEWORK FOR END-TO-END AUTONOMOUS DRIVING

Yongkang Li[1,2 *], **Kaixin Xiong**[2 *], **Xiangyu Guo**[1,2], **Fang Li**[2], **Sixu Yan**[1], **Gangwei Xu**[1,2], **Lijun Zhou**[2], **Long Chen**[2], **Haiyang Sun**[2 †], **Bing Wang**[2], **Kun Ma**[2], **Guang Chen**[2], **Hangjun Ye**[2], **Wenyu Liu**[1], **Xinggang Wang**[1 ✉]

[1]Huazhong University of Science and Technology [2]Xiaomi EV
[*]{liyk, xgwang}@hust.edu.cn, {sunhaiyang1}@xiaomi.com
Model & Data: ReCogDrive HuggingFace Collection
Code: ReCogDrive Github Repository

ABSTRACT

Recent studies have explored leveraging the world knowledge and cognitive capabilities of Vision-Language Models (VLMs) to address the long-tail problem in end-to-end autonomous driving. However, existing methods typically formulate trajectory planning as a language modeling task, where physical actions are output in the language space, potentially leading to issues such as format-violating outputs, infeasible actions, and slow inference speeds. In this paper, we propose ReCogDrive, a novel **Re**inforced **Cog**nitive framework for end-to-end autonomous **Driv**ing, unifying driving understanding and planning by integrating an autoregressive model with a diffusion planner. First, to instill human driving cognition into the VLM, we introduce a hierarchical data pipeline that mimics the sequential cognitive process of human drivers through three stages: generation, refinement, and quality control. Building on this cognitive foundation, we then address the language-action mismatch by injecting the VLM's learned driving priors into a diffusion planner to efficiently generate continuous and stable trajectories. Furthermore, to enhance driving safety and reduce collisions, we introduce a Diffusion Group Relative Policy Optimization (DiffGRPO) stage, reinforcing the planner for enhanced safety and comfort. Extensive experiments on the NAVSIM and Bench2Drive benchmarks demonstrate that ReCogDrive achieves state-of-the-art performance. Additionally, qualitative results across diverse driving scenarios and DriveBench highlight the model's scene comprehension.

1 INTRODUCTION

Autonomous driving, which aims to predict a smooth, comfortable, and collision-free trajectory for a vehicle, has seen significant advancements. Recent end-to-end autonomous driving systems (Jiang et al., 2023; Hu et al., 2023; Chen et al., 2024b; Hu et al., 2022; Zhang et al., 2024a) unify the perception (Jiang et al., 2024b; Philion & Fidler, 2020; Zhang et al., 2023), prediction (Chai et al., 2019; Gu et al., 2023), and planning (Chitta et al., 2022; Liao et al., 2024) modules into a single pipeline for joint optimization, demonstrating impressive performance under open-loop evaluation. However, these systems often fail to generalize to long-tail scenarios, where data is limited and the driving conditions deviate significantly from those encountered during training.

Recent research (Tian et al., 2024; Jiang et al., 2024a; Hwang et al., 2024) addresses the long-tail challenge by introducing VLMs, which are pre-trained on large-scale internet datasets and exhibit strong generalization abilities along with rich world knowledge. Specifically, VLMs applications in autonomous driving can be categorized into two main approaches: (1) *dual-system* approaches (Jiang et al., 2024a; Tian et al., 2024), where VLMs generate low-frequency trajectories or high-level commands to guide an end-to-end driving system; and (2) *single-system* approaches (Hwang et al.,

[*]This work was done when Yongkang Li was an intern at Xiaomi EV. [*] Equal contribution. [†] Project leader.
✉ Corresponding author: xgwang@hust.edu.cn.

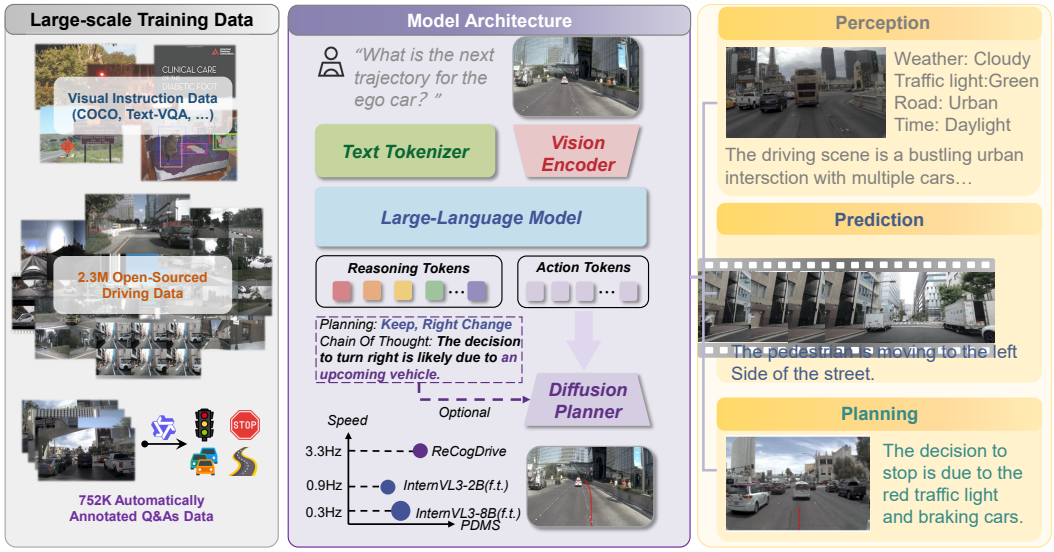

Figure 1: **Overview of ReCogDrive.** We present ReCogDrive, an end-to-end autonomous driving system, which possesses rich driving priors and generates continuous, stable trajectories via a diffusion denoising process. ReCogDrive is capable of performing tasks spanning from low-level scene perception and motion prediction to high-level driving planning and decision making.

2024; Mao et al., 2023a; Xing et al., 2024; Mao et al., 2023b; Wang et al., 2024b; Bai et al., 2024; Zhang et al., 2024c; Zhao et al., 2025), where standalone VLMs directly predict future trajectories and can be optimized in an end-to-end manner. Most of these approaches reformulate the motion planning task as a language modeling problem, generating trajectories in a textual format through autoregressive prediction. These methods leverage the generalization of the models and chain-of-thought (Wei et al., 2022) reasoning to enhance interpretability and reasoning in complex scenarios.

Despite these advantages, directly applying pre-trained VLMs by reformulating trajectory planning as a text generation task for autonomous driving reveals three critical limitations: (1) *Domain discrepancy of pre-trained knowledge.* VLMs (Mao et al., 2023a;b) are trained on generic internet data that lacks the nuanced knowledge required for driving, resulting in a significant domain gap. (2) *Modality mismatch in trajectory generation.* The discrete language space of VLMs fundamentally conflicts with the continuous action space required for planning. This mismatch leads to practical issues, as the probabilistic nature of autoregressive decoding can lead not only to physically infeasible trajectories but also to format-violating outputs that result in parsing errors. (3) *Suboptimal policies from imitation learning.* The heavy reliance on behavior cloning causes models (Hwang et al., 2024) to converge to a suboptimal policy that struggles in rare scenarios and can be unsafe.

To address these challenges, we propose ReCogDrive, a novel end-to-end autonomous driving system that integrates the cognitive reasoning of Vision-Language Models (VLMs) with a reinforcement learning-enhanced diffusion planner. Our framework introduces three key innovations: First, to bridge the domain gap, we design a hierarchical data pipeline that, through three stages of generation, refinement, and quality control, constructs a large-scale VQA dataset to instill human-like cognitive priors into the VLM. Second, to resolve the modality mismatch, we design a diffusion planner that effectively translates the VLM's latent cognitive representations into continuous and stable driving trajectories. Finally, to overcome the limitations of imitation learning, we introduce a reinforcement learning stage based on Diffusion Group Relative Policy Optimization (DiffGRPO), enabling the planner to explore safer, more optimal behaviors beyond the expert dataset.

We extensively evaluate ReCogDrive on NAVSIM and Bench2Drive, achieving new state-of-the-art performance in both open-loop and closed-loop settings. Additionally, we test ReCogDrive-VLM on the DriveLM and DriveBench benchmarks, demonstrating its superiority over both closed-source generalist models and open-source expert models. Qualitative analyses further demonstrate that our reinforcement learning method enables the model to drive more safely and comfortably while significantly reducing collisions. The main contributions of this work are as follows:

- We propose ReCogDrive, a novel end-to-end autonomous driving framework that integrates a cognitive VLM with a diffusion planner, leveraging the rich world knowledge of VLMs to provide cognitive guidance and enabling stable and precise trajectory generation.
- We propose Diffusion Group Relative Policy Optimization (DiffGRPO) to fine-tune the planner, allowing the model to learn directly from experience and optimize for safety and comfort, moving beyond mere imitation.
- We establish new state-of-the-art performance on NAVSIM and Bench2Drive in both open-loop and closed-loop evaluations, demonstrating significant improvements over prior approaches.

2 Related Work

Vision-Language-Models in Autonomous Driving. Numerous studies have leveraged the world knowledge embedded in VLMs to explore their application in autonomous driving. Current approaches for autonomous driving using VLMs can be categorized primarily into two types: *dual-system* (Tian et al., 2024; Jiang et al., 2024a) and *single-system* (Hwang et al., 2024; Mao et al., 2023a; Xing et al., 2024; Mao et al., 2023b; Wang et al., 2024b; Bai et al., 2024; Shao et al., 2024a; Zhang et al., 2024c; Zhao et al., 2025; Fu et al., 2025; Zhou et al., 2025a). Dual-system methods, such as DriveVLM and Senna, integrate VLMs with end-to-end driving systems, where VLMs generate low-frequency trajectories or high-level commands that guide the end-to-end model in producing the final trajectory. In addition, several recent approaches (Pan et al., 2024; Hegde et al., 2025) distill VLM knowledge into end-to-end planners, further improving generalization and robustness. In contrast, single-system methods, such as GPT-Driver and EMMA, reformulate the trajectory prediction task as a language modeling problem and leverage chain-of-thought (Wei et al., 2022) to enhance explainability. However, these text-based approaches often suffer from high inference latency and malformed outputs, whereas our ReCogDrive framework combines a VLM with a diffusion planner to produce more stable, safer trajectories while achieving a 3.5× speedup.

Diffusion Models for Policy Learning. The recent success of diffusion models in domains like image generation (Podell et al., 2023; Zheng et al., 2024), robotics (Chi et al., 2023; Liu et al., 2024b; Black et al., 2024; Yan et al., 2025; Bjorck et al., 2025), and traffic simulation (Yang et al., 2024; Zhong et al., 2023; Zeng et al., 2025) has spurred their application in autonomous driving. For instance, DiffusionDrive (Liao et al., 2024) employs truncated diffusion with anchor priors for real-time multimodal planning. GoalFlow (Xing et al., 2025) applies goal-point guidance with flow matching to generate high-quality trajectories. Diffusion Planner (Zheng et al., 2025) redefines planning as a future trajectory generation task, jointly producing plans and motion forecasts. Our approach uses world knowledge from VLMs to guide the diffusion process, thereby improving the model's understanding of driving scenarios.

Reinforcement Learning in Autonomous Driving. Reinforcement Learning has proven effective in games (Hafner et al., 2023), robotics (Ren et al., 2024), and LLMs (Guo et al., 2025). Recently, many studies have introduced reinforcement learning into autonomous driving to improve model generalization. RAD (Gao et al., 2025) proposes training an end-to-end AD agent using Reinforcement Learning in a photorealistic 3DGS environment. CarPlanner (Zhang et al., 2025) learns an auto-regressive policy for consistent multi-modal trajectories, outperforming imitation learning. AlphaDrive (Jiang et al., 2025), R2SE (Liu et al., 2025), Drive-R1 Li et al. (2025c) and TrajHF (Li et al., 2025a) incorporate GRPO to enhance the generalization of driving policies. Gen-Drive (Huang et al., 2025) combines diffusion models with RL and reward modeling for better policies. Our method novelly employs a Diffusion Group Relative Policy Optimization (DiffGRPO) scheme to fine-tune Vision-Language-Action (VLA) models and enhance their planning capabilities.

3 Preliminaries

Problem Definition. Autonomous driving aims to predict smooth and collision-free trajectory in future seconds, given the ego status S_{ego} (e.g., ego speed $\in \mathbb{R}^2$ containing v_x, v_y and ego acceleration $\in \mathbb{R}^2$ containing a_x, a_y), the historical ego trajectory $I_{\text{hist}} \in \mathbb{R}^{T_{\text{hist}} \times 3}$ (containing past waypoints and headings), sensor input $I_{\text{cam}} \in \mathbb{R}^{K \times V \times H \times W \times 3}$ (containing current and historical K frames from V camera views), and navigation information L_{nav} (High-level command such as "go straight").

Conventional end-to-end driving algorithm Φ formulate this as

$$\mathbf{V}_{\text{traj}} = \Phi\big(I_{\text{cam}},\, I_{\text{hist}},\, L_{\text{nav}},\, S_{\text{ego}}\big), \tag{1}$$

where $\mathbf{V}_{\text{traj}}$ denotes the planned future trajectory, parameterized as $\{(x_t, y_t, \theta_t)\}_{t=1}^{T} \in \mathbb{R}^{T\times 3}$, with (x_t, y_t) the 2D waypoints and θ_t the corresponding heading angles. Explicit headings are needed to construct oriented ego polygons for collision evaluation and to derive yaw-related comfort measures, which cannot be robustly obtained from sparsely sampled waypoints alone. While methods such as (Hu et al., 2023; Jiang et al., 2023; Liao et al., 2024; Chen et al., 2024b) have shown strong effectiveness, their black-box nature impedes interpretability and they often fail to generalize to rare corner cases in real-world driving.

Recent works (Hwang et al., 2024; Mao et al., 2023a; Zhang et al., 2024b) utilize the rich world knowledge and causal reasoning capabilities of Vision–Language Models for autonomous driving. VLMs output trajectories in textual form and generate explicit reasoning processes:

$$T_{\text{traj}},\, T_{\text{reason}} = \text{VLM}\big(I_{\text{cam}},\, I_{\text{hist}},\, L_{\text{nav}},\, S_{\text{ego}}\big). \tag{2}$$

However, we observe an inherent mismatch between the language-formatted trajectory space and the continuous action space, and the autoregressive decoding process can suffer from output collapse, leading to erroneous trajectories.

Diffusion Policy. Denoising Diffusion Probabilistic Models (DDPMs) (Ho et al., 2020; Nichol & Dhariwal, 2021) learn a generative model by reversing a fixed, Markovian noising process that gradually corrupts data with Gaussian noise. Given a clean trajectory $\mathbf{x}_0$, the forward process defines:

$$q(\mathbf{x}_t \mid \mathbf{x}_{t-1}) = \mathcal{N}\big(\mathbf{x}_t;\, \sqrt{1-\sigma_t^2}\,\mathbf{x}_{t-1},\, \sigma_t^2\mathbf{I}\big), \quad t = 1, \ldots, T, \tag{3}$$

where σ_t is the noise standard deviation at step t. At inference, trajectories are generated by initializing $\mathbf{x}_T \sim \mathcal{N}(\mathbf{0}, \mathbf{I})$ and iteratively denoising:

$$\mathbf{x}_{t-1} = \frac{1}{\sqrt{1-\sigma_t^2}}\Big(\mathbf{x}_t - \sigma_t^2\,\epsilon_\theta(\mathbf{x}_t, t)\Big) + \sigma_t\,\mathbf{z}, \quad \mathbf{z} \sim \mathcal{N}(0, \mathbf{I}). \tag{4}$$

Denoting trajectory waypoint as $\mathbf{x}_0$, this framework naturally extends to trajectory-level policy generation, where the denoising network ϵ_θ learns to refine noisy motion plans into smooth trajectories.

4 Methodology

In this section, we present the overall framework and training paradigm of ReCogDrive. First, we introduce a scalable hierarchical data pipeline that curates a multi-level cognitive dataset spanning from perception to reasoning to instill the VLM with nuanced, human-like driving priors. Second, we detail our cognition-guided diffusion planner, a novel architecture that resolves the modality mismatch by translating the VLM's latent semantic representations into continuous and stable trajectories. Finally, we describe our policy refinement stage, where a Diffusion Group Relative Policy Optimization (DiffGRPO) algorithm is employed to fine-tune the planner with simulated rewards, optimizing for safety and comfort beyond the confines of the expert dataset.

4.1 Scalable Hierarchical Data Pipeline For Driving Pretraining

To bridge the gap between general Vision-Language Models (VLMs) and autonomous driving, we introduce a scalable, structured pipeline for the automated generation of high-fidelity driving data, as shown in Fig. 2. This pipeline comprises three stages: Generation, Refinement, and Quality Control.

In the Generation stage, we align with the sequential cognitive process of human drivers, organized into four levels: *(1) Foundational Perception:* constructing representations of static and dynamic scene elements; *(2) Dynamic Understanding:* analyzing multi-agent dynamics and predicting near-term behaviors of surrounding entities; *(3) Planning and Reasoning:* formulating executable, safety-aware driving plans and providing concise rationales; and *(4) Advanced Reasoning:* conducting counterfactual analyses and fine-grained trade-off evaluations. To achieve this, we combine ground-truth data for objective tasks with a state-of-the-art VLM for subjective annotations.

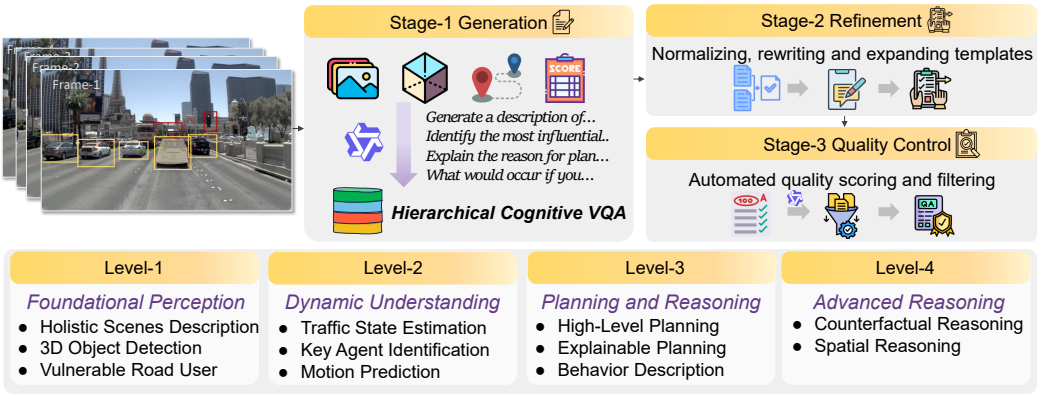

Figure 2: **Overview of our Scalable Hierarchical Data Pipeline.** We employ a three-stage process of Generation, Refinement, and Quality Control to produce a high-quality dataset that mimics the cognitive process of a human driver.

The Refinement stage integrates open-source datasets, followed by normalization, rewriting, and question-template augmentation to ensure linguistic and semantic consistency. Finally, the Quality Control stage applies automated scoring and rigorous filtering based on linguistic accuracy, visual clarity, etc., retaining only the high quality samples. This systematic design ensures our pre-training dataset is both reliable and scalable, enabling the adaptation of a general VLM into a domain-specialized cognitive model for autonomous driving.

4.2 Cognition-Guided Diffusion Planner

While autoregressive paradigms offer a straightforward way to generate trajectories in textual form, they suffer from inherent limitations: (i) the mismatch between discrete language space and continuous action space often leads to infeasible or jerky trajectories, and (ii) VLMs are prone to hallucination and decoding errors, which compromise safety in autonomous driving. To address these issues, we propose a *Cognition-Guided Diffusion Planner*, which integrates human cognitive driving priors from a VLM with a diffusion planner to generate smooth and safety-aware trajectories. Formally, given a noisy trajectory sample $\mathbf{x}_t \in \mathbb{R}^{N\times 3}$, the denoising step is defined as:

$$\mathbf{x}_{t-1} = D_{\text{act}}\Big(\text{DiT}_\theta(z_t;\, F_h;\, S_{\text{ego}};\, t)\Big), \quad z_t = \text{concat}\big(E_{\text{act}}(\mathbf{x}_t),\, E_{\text{his}}(I_{\text{hist}}),\, \bar{F}_h\big)\,, \tag{5}$$

where F_h denotes the VLM hidden states, S_{ego} represents the ego-vehicle status, and z_t is the fused latent combining the noisy-action latent from the action encoder E_{act}, the historical-trajectory latent of I_{hist} encoded by the history-trajectory encoder E_{his}, and the semantic prior $\bar{F}_h$ obtained by mean-pooling over F_h. And D_{act} is the action decoder that predicts the next step noisy trajectory. The diffusion model is trained by minimizing:

$$\mathcal{L}_{\text{dif}} = \mathbb{E}_{z_t,c}\,\|\epsilon - \epsilon_\pi(z_t, c)\|^2\,, \tag{6}$$

with $\epsilon \sim \mathcal{N}(0, \mathbf{I})$ and condition $c = \{F_h, S_{\text{ego}}\}$.

Vision-Language Model Guidance. We adopt InternVL3 (Zhu et al., 2025; Chen et al., 2024e) as the cognitive backbone for its strong multi-modal reasoning. The VLM encodes multi-view images and textual queries into hidden states $F_h \in \mathbb{R}^{L\times D}$, which act as cognitive tokens carrying driving priors and serve as cross-attention conditions in the diffusion transformer. We further obtain a global semantic embedding $\bar{F}_h$ via average pooling over F_h, providing stable contextual guidance during denoising. Additionally, the VLM can optionally output high-level driving instructions and chain-of-thought reasoning to enhance trajectory generation.

Diffusion Transformer Design. Our diffusion planner builds on DiT (Peebles & Xie, 2023; Yao et al., 2025) blocks, enhanced with lightweight but effective design choices: SwiGLU FFN (Shazeer, 2020) for expressive non-linearity, RoPE (Su et al., 2024) for relative positional encoding, and both

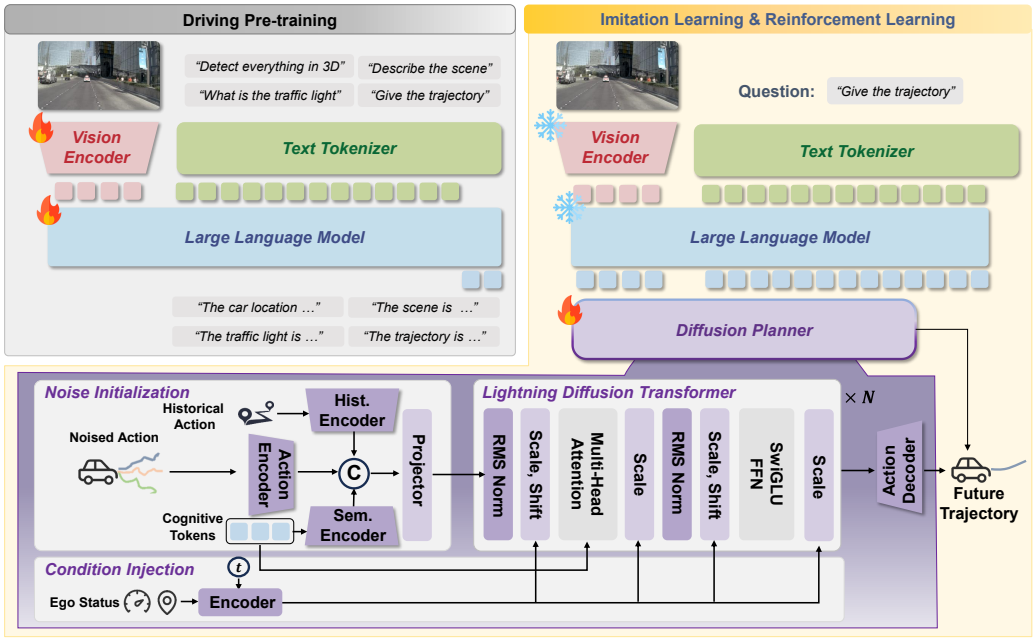

Figure 3: **Training Pipeline and Model Architecture.** ReCogDrive couples a VLM with a diffusion planner: the VLM encodes inputs into cognitive tokens guiding trajectory denoising. Training follows three stages: Driving Pre-training, imitation learning, and reinforcement learning.

QK-Norm and RMSNorm (Zhang & Sennrich, 2019) for stable optimization. Each block alternates between (i) *self-attention*, which models pairwise waypoint relations, and (ii) *cross-attention*, which injects semantic priors F_h into the trajectory space. This design enables a structured fusion of scene-level cognition with low-level trajectory optimization.

Historical and Ego Information Fusion. To capture temporal consistency, historical trajectories $\mathbf{x}_{\text{hist}}$ are encoded and concatenated with the noisy trajectory embeddings. Ego-vehicle status S_{ego} (e.g., speed, acceleration) is injected via *AdaLN modulation*, ensuring that the planner is conditioned on the vehicle's physical state. This dual conditioning mechanism enhances stability, safety, and adaptability in diverse driving scenarios.

4.3 Diffusion Group Relative Policy Optimization

Relying solely on imitation learning exhibits fundamental limitations (Chu et al., 2025; Osa et al., 2018; Ren et al., 2024), since expert demonstrations may be multi-modal, leading to conflictual optimization results. As shown in Fig. 4(a), when trained in this rare intersection turn scenario with multiple expert trajectories, the model resorts to learning an average trajectory to achieve global optimality, which can lead to incorrect or unsafe maneuvers. Consequently, even though the diffusion planner trained through imitation learning closely matches expert trajectories in terms of displacement, it still frequently produces collisions or drives outside the drivable area.

To enable exploration beyond imitation, we introduce *DiffGRPO*, a Group Relative Policy Optimization algorithm specifically designed for diffusion planners that tightly couples GRPO (Shao et al., 2024b) with the denoising process. We adopt GRPO since it naturally samples multiple candidate trajectories, which aligns with autonomous driving where multiple feasible ground truth trajectories can satisfy the same scene and high level intent. Following (Ren et al., 2024), we interpret the diffusion policy π_θ as an internal Markov decision process: starting from Gaussian noise, the model gradually denoises to generate a full trajectory. Concretely, we sample G trajectories, each represented by a diffusion chain:

$$\mathbf{x} = (x_T,\, x_{T-1},\, \ldots,\, x_0), \tag{7}$$

where T is the total number of denoising steps and transitions follow:

$$x_T \sim \mathcal{N}(0, \mathbf{I}), \qquad x_{t-1} \sim \pi_\theta(x_{t-1} \mid x_t). \tag{8}$$

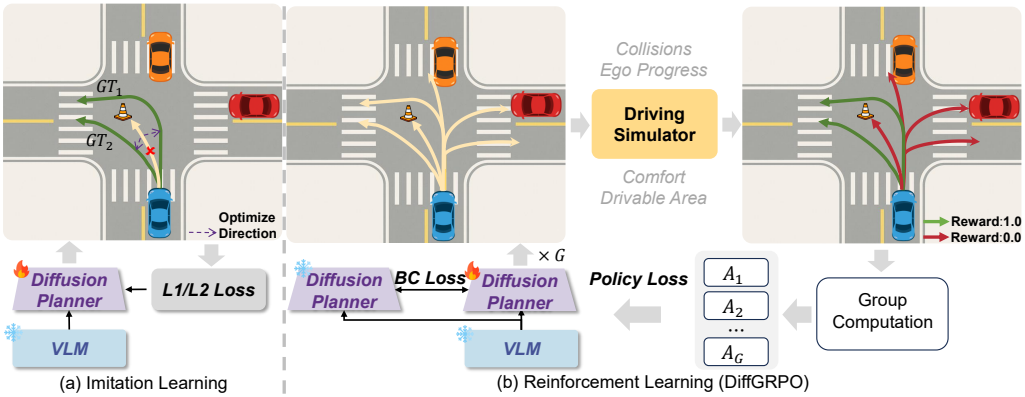

Figure 4: **Comparison of Training Paradigms.** (a) **Imitation Learning:** the diffusion planner is trained offline to mimic ground truth trajectories using L1/L2 losses, but tends to learn averaged, suboptimal paths. (b) **Reinforcement Learning:** multiple trajectories are sampled and evaluated in the NAVSIM simulator, scored on collision avoidance, drivable area compliance and other metrics, and advantages are computed via group computation to update the diffusion planner.

Unlike prior approaches (Li et al., 2025a;c) that rely on simple ℓ_2 trajectory distances as surrogate rewards, we leverage the NAVSIM simulator to providing realistic feedback on safety and comfort. Each rollout is evaluated in terms of collisions, drivable-area compliance, and driving comfort, with the results aggregated into a Predictive Driver Model Score (PDMS) that serves as the reward r_i. We cast this as a single-step decision, treating the whole trajectory as one composite action with its PDMS score as the reward. We then compute the group-standardized advantage:

$$\hat{A}_i = \frac{r_i - \mu}{\sigma}, \quad \mu = \frac{1}{G}\sum_{j=1}^{G} r_j, \quad \sigma^2 = \frac{1}{G}\sum_{j=1}^{G}(r_j - \mu)^2, \quad i = 1, \ldots, G. \tag{9}$$

Each conditional step in the diffusion chain is a Gaussian policy:

$$\pi_\theta(x_{t-1} \mid x_t) = \mathcal{N}\Big(x_{t-1};\, \mu_\theta(x_t, t),\, \sigma_t^2 I\Big), \tag{10}$$

where $\mu_\theta(x_t, t)$ is the model-predicted mean and $\sigma_t^2 I$ the (fixed) covariance. Thus, the probability density of the full chain $\mathbf{x}_{0:T}$ under π_θ, where $p(x_T)$ is a Gaussian prior independent of θ, is:

$$\log \pi_\theta(\mathbf{x}_{0:T}) = \log p(x_T) + \sum_{t=1}^{T} \log \pi_\theta(x_{t-1} \mid x_t), \tag{11}$$

Finally, we compute the policy loss following (Williams, 1992; Shao et al., 2024b) while concurrently incorporating a behavior cloning loss to prevent collapse during exploration.

$$L = \underbrace{-\frac{1}{G}\sum_{i=1}^{G}\frac{1}{T}\sum_{t=1}^{T}\gamma^{t-1}\log \pi_\theta\big(x_{t-1}^{(i)} \mid x_t^{(i)}\big)\,\hat{A}_i}_{L_{\mathrm{RL}}} - \underbrace{\lambda\,\frac{1}{G}\sum_{i=1}^{G}\frac{1}{T}\sum_{t=1}^{T}\log \pi_\theta\big(\tilde{x}_{t-1}^{(i)} \mid \tilde{x}_t^{(i)}\big)}_{L_{\mathrm{BC}}}, \tag{12}$$

where γ is the discount coefficient mitigating instability in early denoising steps, λ is the weight for the behavior cloning loss, and $\tilde{x}_{t-1}, \tilde{x}_t$ are values sampled from the reference policy π_{ref}. We omit the PPO-style clipping and set the update iteration to 1, so $\pi = \pi_{\mathrm{old}}$. Through DiffGRPO, the diffusion planner learns to generate safe and comfortable trajectories in closed-loop settings, going beyond mere imitation and enhancing the robustness of our framework.

Table 1: **Performance comparison on NAVSIM *navtest* using closed-loop metrics.** † denotes models fine-tuned on the NAVSIM trajectory dataset.

Method	Image	Lidar	NC↑	DAC↑	TTC↑	Comf. ↑	EP↑	PDMS↑
Constant Velocity			68.0	57.8	50.0	**100**	19.4	20.6
Ego Status MLP			93.0	77.3	83.6	**100**	62.8	65.6
VADv2-$\mathcal{V}_{8192}$ (Chen et al., 2024b)	✓		97.2	89.1	91.6	**100**	76.0	80.9
DrivingGPT (Chen et al., 2024c)	✓		**98.9**	90.7	94.9	95.6	79.7	82.4
UniAD (Hu et al., 2023)	✓		97.8	91.9	92.9	**100**	78.8	83.4
TransFuser (Chitta et al., 2022)	✓	✓	97.7	92.8	92.8	**100**	79.2	84.0
PARA-Drive (Weng et al., 2024)	✓		97.9	92.4	93.0	99.8	79.3	84.0
DRAMA (Yuan et al., 2024)	✓	✓	98.0	93.1	94.8	**100**	80.1	85.5
Hydra-MDP-$\mathcal{V}_{8192}$-W-EP (Li et al., 2024)	✓	✓	98.3	96.0	94.6	**100**	78.7	86.5
DiffusionDrive (Liao et al., 2024)	✓	✓	98.2	96.2	94.7	**100**	82.2	88.1
WoTE (Li et al., 2025b)	✓	✓	98.5	96.8	**94.9**	99.9	81.9	88.3
VLMs-based Methods								
QwenVL2.5-8B† (Bai et al., 2025)	✓		97.8	92.1	92.8	**100**	78.3	83.3
InternVL3-8B† (Zhu et al., 2025)	✓		97.0	92.4	91.8	**100**	78.9	83.3
AutoVLA Zhou et al. (2025b)	✓		98.4	95.6	**98.0**	99.9	81.9	89.1
ReCogDrive(ours)	✓		97.9	**97.3**	94.9	**100**	**87.3**	**90.8**

Table 2: **Closed-loop and Multi-ability Testing Results in CARLA Bench2Drive Leaderboard.**

Method	**Closed-loop Metric** ↑				**Multi-Ability Test** (%) ↑					
	Efficiency	Comfort	Success	**DS**	Merging	Overtaking	Emerg. Brake	GiveWay	Traf. Sign	**Mean**
TCP* (Wu et al., 2022)	54.26	47.80	15.00	40.70	16.18	20.00	20.00	10.00	6.99	14.63
TCP-ctrl* (Wu et al., 2022)	55.97	**51.51**	7.27	30.47	10.29	4.44	10.00	10.00	6.45	8.23
TCP-traj* (Wu et al., 2022)	76.54	18.08	30.00	59.90	8.89	24.29	51.67	40.00	46.28	34.22
TCP-traj w/o distill. (Wu et al., 2022)	78.78	22.96	30.05	49.30	17.14	6.67	40.00	40.00	28.72	28.51
ThinkTwice (Jia et al., 2023b)	76.93	16.22	3.13	62.44	27.38	18.42	35.82	**50.00**	54.23	37.17
DriveAdapter* (Jia et al., 2023a)	70.22	16.01	33.08	64.22	28.82	26.38	48.76	**50.00**	56.43	**42.08**
AD-MLP (Zhai et al., 2023)	48.45	22.63	0.00	18.05	0.00	0.00	0.00	0.00	4.35	0.87
UniAD-T. (Hu et al., 2023)	123.92	47.04	13.18	40.73	8.89	9.33	20.00	20.00	15.43	14.73
UniAD-B. (Hu et al., 2023)	129.21	43.58	16.36	45.81	14.10	17.78	21.67	10.00	14.21	15.55
VAD (Jiang et al., 2023)	**157.94**	46.01	15.00	42.35	8.11	24.44	18.64	20.00	19.15	18.07
DriveTransformer-L. (Jia et al., 2025)	100.64	46.01	35.01	63.46	17.57	**35.00**	48.36	40.00	52.10	38.60
ReCogDrive	138.18	17.45	**45.45**	**71.36**	**29.73**	20.00	**69.09**	20.00	**71.34**	42.03

5 EXPERIMENTS

5.1 EXPERIMENTAL SETUP.

Implementation Details. We choose InternVL3 (Zhu et al., 2025), comprising a 300M-parameter InternViT visual encoder (Chen et al., 2024e) and a Qwen2.5 Large-Language-Model (Bai et al., 2025), as our base model, which demonstrates strong performance on multiple benchmarks. Images are processed through a dynamic resolution preprocessing strategy. In the first stage, we conduct supervised fine-tuning (SFT) on the VLM using the dataset constructed by our hierarchical data pipeline for three epochs. In the second stage, with the VLM parameters frozen, we train the diffusion model via DDPM for 200 epochs. In the third stage, we further optimize the diffusion model using reinforcement learning for 10 epochs, with one policy update per batch. The datasets and training hyperparameters for all three stages are described in detail in the supplementary material.

Dataset. We evaluate primarily on two challenging benchmarks: NAVSIM (Dauner et al., 2025) and Bench2Drive (Jia et al., 2024). NAVSIM is a planning-oriented autonomous driving dataset built on OpenScene (Contributors, 2023), a redistribution of nuPlan (Caesar et al., 2021). The dataset is split into *navtrain* (1,192 training scenes) and *navtest* (136 evaluation scenes). Bench2Drive is a CARLA-based benchmark composed of 220 short routes, each containing a distinct, safety-critical scenario. In addition, to build the VLM's cognitive foundation, ReCogDrive is trained on a collection of VQA datasets, including DriveLM (Sima et al., 2024) and LingoQA (Marcu et al., 2024), with further details provided in the supplementary material.

Table 3: **Ablation study on the proposed components of ReCogDrive.** We evaluate the effect of driving pre-training, diffusion planner, and reinforcement learning on NAVSIM evaluation.

ID	Trajectory training	Driving Pre-training	Diffusion Planner	Diff GRPO	NC	DAC	TTC	Conf.	EP	PDMS
1	✓	✗	✗	✗	97.4	91.3	93.0	100	77.2	82.4
2	✓	✓	✗	✗	97.6	93.1	92.7	100	79.1	84.1
3	✓	✓	✓	✗	98.1	94.7	94.2	100	80.9	86.5
4	✓	✓	✓	✓	97.9	97.3	94.9	100	87.3	90.8

Table 4: Comparison of trajectory generation methods.† indicates inference with `lmdeploy`.

Method	Time (s)	PDMS ↑	Err. (%) ↓
VLM Plain Text†	1.0702	84.1	0.01
VLM + MLP	0.3045	75.5	0.00
VLM + Query-based Decoder	0.3050	85.0	0.00
VLM + Vanilla Diffusion	0.3060	85.4	0.00
+ *SwiGLU FFN*	0.3065	85.7	0.00
+ *RMS Norm*	0.3070	85.8	0.00
+ *RoPE & QK Norm*	0.3061	86.5	0.00

Table 5: Model performance on Drive VQA Benchmark.

Method	DriveLM	DriveBench				
	GPT-Score	Percep.	Predict.	Plan.	Behav.	Avg.
LLaVA-1.5	61.91	23.22	22.02	29.15	13.60	22.00
InternVL2	64.13	32.36	45.52	53.27	54.58	46.43
Qwen2-VL	–	30.13	49.35	61.30	51.26	48.01
DriveLM	65.25	16.85	44.33	68.71	42.78	43.17
Dolphins	–	9.59	32.66	52.91	8.81	25.99
GPT-4o	67.27	35.37	51.30	75.75	45.40	51.96
ReCogDrive	**67.30**	64.95	49.34	70.20	42.36	**56.71**

Table 6: **Comparison of different RL algorithms.** We evaluate REINFORCE, DPPO, and DiffGRPO on our diffusion planner under the same training and evaluation setting.

Algorithm	NC	DAC	TTC	Conf.	EP	PDMS
REINFORCE	98.5	97.3	95.9	100	82.9	89.5
DPPO	98.6	97.6	96.0	100	82.4	89.5
DiffGRPO	97.9	97.3	94.9	100	87.3	**90.8**

Figure 5: **Training curves on NAVSIM.**

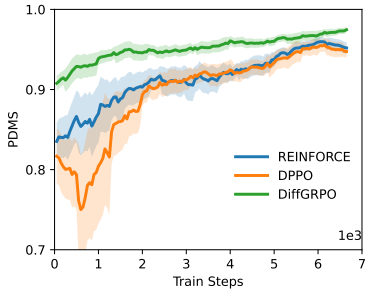

5.2 Main Results and Ablation Study

Experiments on the NAVSIM Benchmark. Tab. 1 reports results on NAVSIM. ReCogDrive achieves a PDMS of 90.8, establishing a new state-of-the-art. Remarkably, it outperforms DiffusionDrive (Liao et al., 2024) and WoTE (Li et al., 2025b), both of which use camera and LiDAR inputs, by 2.7 and 2.5 PDMS, respectively, while using only camera input. Compared with our reproduced InternVL3 (Zhu et al., 2025) and QwenVL2.5 (Bai et al., 2025) trained directly on NAVSIM trajectories, ReCogDrive improves PDMS by 7.5, validating the effectiveness of our training paradigm. It also surpasses the prior vision-only state-of-the-art, PARA-Drive (Weng et al., 2024), by 6.8 PDMS.

Bench2Drive Closed-loop Performance. Tab. 2 reports closed-loop and multi-ability results on the CARLA Bench2Drive leaderboard. ReCogDrive achieves the highest scenario success rate of 45.45% and the top Driving Score of 71.36, surpassing prior end-to-end baselines. It also excels in safety-critical skills such as emergency braking 69.09% and traffic sign compliance 71.34, while maintaining strong efficiency and a competitive multi-ability mean of 42.03. These results highlight the effectiveness and reliability of our framework in complex urban driving.

Ablation study on ReCogDrive. Tab. 3 presents an ablation study on the proposed components of ReCogDrive. When training InternVL3 solely on NAVSIM trajectory data, the model achieves a PDMS of 83.3. Adapting the VLM to driving scenarios with our large-scale driving QA data increases PDMS by 1.7. Introducing the diffusion planner for continuous trajectory prediction further raises PDMS by 2.4. Finally, DiffGRPO achieves a PDMS of 90.8 with a 4.3 improvement, demonstrating the effectiveness of our RL scheme in producing safer driving behavior.

Comparison of Trajectory Generation Methods. We compare trajectory generation methods in terms of inference speed, PDM Score, and error rate as shown in Tab. 4. The error rate quantifies the

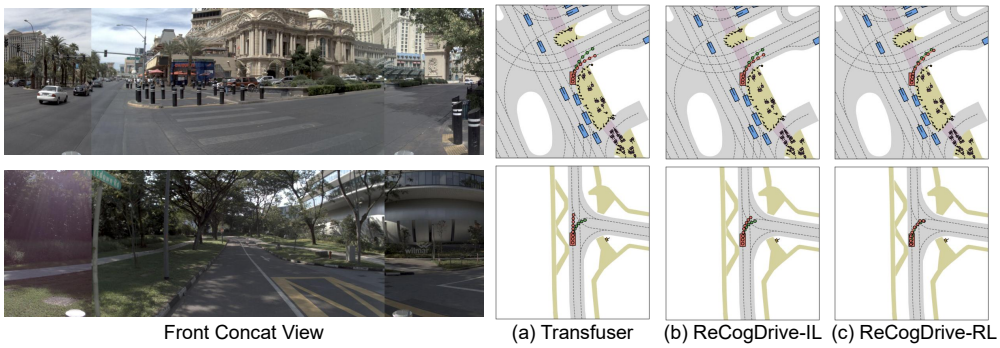

Figure 6: **Comparisons on the Navtest benchmark.**

occurrence of malformed outputs that lack a parsable trajectory, which constitutes a low-probability failure mode in direct trajectory regression using VLMs. All inference times in Tab. 4 are measured as end-to-end wall-clock latency for processing a single sample.

Generating trajectories as plain text is slow due to the autoregressive process and may suffer from format errors that compromise safety. In contrast, MLP, Query-based Decoder (Chitta et al., 2022), and diffusion planner are substantially faster, with diffusion-based approaches further boosting PDMS. Building on this, we integrated lightweight architectural refinements including SwiGLU FFN, RMS Norm, RoPE, and QK Norm. Our final model ReCogDrive achieves a 3.5× speedup and a 2.4 PDMS gain over the text baseline, validating the effectiveness of our design.

Evaluation on Drive VQA Benchmarks. To provide a comprehensive assessment of our model's language-related capabilities in driving scenarios, we evaluate its performance on the DriveLM and DriveBench benchmarks. The results, presented in Tab. 5, demonstrate the effectiveness of our approach. Our model, ReCogDrive, achieves state-of-the-art performance, surpassing the powerful closed-source GPT-4o model on most key metrics, including the overall DriveBench average score. Furthermore, ReCogDrive significantly outperforms several specialized open-source driving models, validating its strong visual question answering and reasoning abilities in this domain.

Comparison of RL Algorithms for Diffusion Planning. To validate DiffGRPO, we compare it with DPPO (Ren et al., 2024) and REINFORCE (Williams, 1992) using the same diffusion planner and PDMS reward, with results in Tab. 6. Since DiffGRPO samples a group of candidate trajectories under the same scene condition, it naturally matches autonomous driving where a single scene often admits multiple safe ground-truth trajectories, and the group-relative advantage encourages safer and more stable rollouts. As reflected by the training curves, DiffGRPO achieves the best PDMS while converging faster and more stably than DPPO and REINFORCE.

Qualitative Results. In Fig. 6, we compare ReCogDrive (IL and RL) with Transfuser (Chitta et al., 2022), where RL yields safer and more reliable trajectories in challenging turning scenarios. More visualizations are in the supplementary material.

6 Conclusion

In this work, we proposed ReCogDrive, a novel reinforced cognitive framework for end-to-end autonomous driving that integrates a Vision-Language Model with a diffusion planner. We first introduced a scalable hierarchical data pipeline that mimics human driving cognition to construct a foundation model with strong driving priors. Building on this foundation, we designed a cognition-guided diffusion planner that injects VLM-derived cognitive tokens into the denoising process, enabling the generation of continuous, stable, and human-like trajectories. To further refine planning behavior, we introduced DiffGRPO, a reinforcement learning scheme that explicitly optimizes safety and comfort in closed-loop driving. Extensive experiments on multiple benchmarks demonstrate that ReCogDrive achieves state-of-the-art performance, validating the effectiveness of our approach. We hope our work can advance the development of autonomous driving VLAs.

ACKNOWLEDGMENTS AND DISCLOSURE OF FUNDING

This work was partially supported by the National Natural Science Foundation of China under Grant U25B2067.

ETHICS STATEMENT

We acknowledge and adhere to the ICLR Code of Ethics throughout this work. Our research does not involve human subjects or sensitive personal data, and all experiments were conducted in compliance with ethical research practices.

REPRODUCIBILITY STATEMENT

We have made extensive efforts to ensure reproducibility. In the supplementary materials, we provide details of our training datasets, including composition and preprocessing steps in Appx. D. We further include hyperparameters and training details in Appx. E. In addition, we provide our model code as part of the supplementary materials to facilitate reproduction of our results.

REFERENCES

Marah Abdin, Jyoti Aneja, Harkirat Behl, Sébastien Bubeck, Ronen Eldan, Suriya Gunasekar, Michael Harrison, Russell J Hewett, Mojan Javaheripi, Piero Kauffmann, et al. Phi-4 technical report. *arXiv preprint arXiv:2412.08905*, 2024. 20

Shuai Bai, Keqin Chen, Xuejing Liu, Jialin Wang, Wenbin Ge, Sibo Song, Kai Dang, Peng Wang, Shijie Wang, Jun Tang, Humen Zhong, Yuanzhi Zhu, Mingkun Yang, Zhaohai Li, Jianqiang Wan, Pengfei Wang, Wei Ding, Zheren Fu, Yiheng Xu, Jiabo Ye, Xi Zhang, Tianbao Xie, Zesen Cheng, Hang Zhang, Zhibo Yang, Haiyang Xu, and Junyang Lin. Qwen2.5-vl technical report. *arXiv preprint arXiv:2502.13923*, 2025. 8, 9, 22

Yifan Bai, Dongming Wu, Yingfei Liu, Fan Jia, Weixin Mao, Ziheng Zhang, Yucheng Zhao, Jianbing Shen, Xing Wei, Tiancai Wang, et al. Is a 3d-tokenized llm the key to reliable autonomous driving? *arXiv preprint arXiv:2405.18361*, 2024. 2, 3

Johan Bjorck, Fernando Castañeda, Nikita Cherniadev, Xingye Da, Runyu Ding, Linxi Fan, Yu Fang, Dieter Fox, Fengyuan Hu, Spencer Huang, et al. Gr00t n1: An open foundation model for generalist humanoid robots. *arXiv preprint arXiv:2503.14734*, 2025. 3

Kevin Black, Noah Brown, Danny Driess, Adnan Esmail, Michael Equi, Chelsea Finn, Niccolo Fusai, Lachy Groom, Karol Hausman, Brian Ichter, et al. A vision-languageaction flow model for general robot control. *arXiv preprint arXiv:2410.24164*, 2(3):5, 2024. 3

Holger Caesar, Varun Bankiti, Alex H Lang, Sourabh Vora, Venice Erin Liong, Qiang Xu, Anush Krishnan, Yu Pan, Giancarlo Baldan, and Oscar Beijbom. nuscenes: A multimodal dataset for autonomous driving. In *Proceedings of the IEEE/CVF conference on computer vision and pattern recognition*, pp. 11621–11631, 2020. 22

Holger Caesar, Juraj Kabzan, Kok Seang Tan, Whye Kit Fong, Eric Wolff, Alex Lang, Luke Fletcher, Oscar Beijbom, and Sammy Omari. nuplan: A closed-loop ml-based planning benchmark for autonomous vehicles. *arXiv preprint arXiv:2106.11810*, 2021. 8

Xu Cao, Tong Zhou, Yunsheng Ma, Wenqian Ye, Can Cui, Kun Tang, Zhipeng Cao, Kaizhao Liang, Ziran Wang, James M Rehg, et al. Maplm: A real-world large-scale vision-language benchmark for map and traffic scene understanding. In *Proceedings of the IEEE/CVF Conference on Computer Vision and Pattern Recognition*, pp. 21819–21830, 2024. 22, 25

Yuning Chai, Benjamin Sapp, Mayank Bansal, and Dragomir Anguelov. Multipath: Multiple probabilistic anchor trajectory hypotheses for behavior prediction. *arXiv preprint arXiv:1910.05449*, 2019. 1

Kai Chen, Yanze Li, Wenhua Zhang, Yanxin Liu, Pengxiang Li, Ruiyuan Gao, Lanqing Hong, Meng Tian, Xinhai Zhao, Zhenguo Li, et al. Automated evaluation of large vision-language models on self-driving corner cases. *arXiv preprint arXiv:2404.10595*, 2024a. 22, 25

Shaoyu Chen, Bo Jiang, Hao Gao, Bencheng Liao, Qing Xu, Qian Zhang, Chang Huang, Wenyu Liu, and Xinggang Wang. Vadv2: End-to-end vectorized autonomous driving via probabilistic planning. *arXiv preprint arXiv:2402.13243*, 2024b. 1, 4, 8, 19

Yuntao Chen, Yuqi Wang, and Zhaoxiang Zhang. Drivinggpt: Unifying driving world modeling and planning with multi-modal autoregressive transformers. *arXiv preprint arXiv:2412.18607*, 2024c. 8

Zhe Chen, Weiyun Wang, Hao Tian, Shenglong Ye, Zhangwei Gao, Erfei Cui, Wenwen Tong, Kongzhi Hu, Jiapeng Luo, Zheng Ma, et al. How far are we to gpt-4v? closing the gap to commercial multimodal models with open-source suites. *Science China Information Sciences*, 67(12):220101, 2024d. 20

Zhe Chen, Jiannan Wu, Wenhai Wang, Weijie Su, Guo Chen, Sen Xing, Muyan Zhong, Qinglong Zhang, Xizhou Zhu, Lewei Lu, et al. Internvl: Scaling up vision foundation models and aligning for generic visual-linguistic tasks. In *Proceedings of the IEEE/CVF conference on computer vision and pattern recognition*, pp. 24185–24198, 2024e. 5, 8

Cheng Chi, Zhenjia Xu, Siyuan Feng, Eric Cousineau, Yilun Du, Benjamin Burchfiel, Russ Tedrake, and Shuran Song. Diffusion policy: Visuomotor policy learning via action diffusion. *The International Journal of Robotics Research*, pp. 02783649241273668, 2023. 3

Kashyap Chitta, Aditya Prakash, Bernhard Jaeger, Zehao Yu, Katrin Renz, and Andreas Geiger. Transfuser: Imitation with transformer-based sensor fusion for autonomous driving. *IEEE Transactions on Pattern Analysis and Machine Intelligence*, 45(11):12878–12895, 2022. 1, 8, 10, 18, 19

Tianzhe Chu, Yuexiang Zhai, Jihan Yang, Shengbang Tong, Saining Xie, Dale Schuurmans, Quoc V Le, Sergey Levine, and Yi Ma. Sft memorizes, rl generalizes: A comparative study of foundation model post-training. *arXiv preprint arXiv:2501.17161*, 2025. 6

OpenScene Contributors. Openscene: The largest up-to-date 3d occupancy prediction benchmark in autonomous driving. https://github.com/OpenDriveLab/OpenScene, 2023. 8

Daniel Dauner, Marcel Hallgarten, Tianyu Li, Xinshuo Weng, Zhiyu Huang, Zetong Yang, Hongyang Li, Igor Gilitschenski, Boris Ivanovic, Marco Pavone, et al. Navsim: Data-driven non-reactive autonomous vehicle simulation and benchmarking. *Advances in Neural Information Processing Systems*, 37:28706–28719, 2025. 8, 22

Thierry Deruyttere, Simon Vandenhende, Dusan Grujicic, Luc Van Gool, and Marie-Francine Moens. Talk2car: Taking control of your self-driving car. *arXiv preprint arXiv:1909.10838*, 2019. 22, 25

Xinpeng Ding, Jianhua Han, Hang Xu, Xiaodan Liang, Wei Zhang, and Xiaomeng Li. Holistic autonomous driving understanding by bird's-eye-view injected multi-modal large models. In *Proceedings of the IEEE/CVF Conference on Computer Vision and Pattern Recognition*, pp. 13668–13677, 2024. 22, 23, 25

Renju Feng, Ning Xi, Duanfeng Chu, Rukang Wang, Zejian Deng, Anzheng Wang, Liping Lu, Jinxiang Wang, and Yanjun Huang. Artemis: Autoregressive end-to-end trajectory planning with mixture of experts for autonomous driving. *arXiv preprint arXiv:2504.19580*, 2025. 19, 20

Haoyu Fu, Diankun Zhang, Zongchuang Zhao, Jianfeng Cui, Dingkang Liang, Chong Zhang, Dingyuan Zhang, Hongwei Xie, Bing Wang, and Xiang Bai. Orion: A holistic end-to-end autonomous driving framework by vision-language instructed action generation. *arXiv preprint arXiv:2503.19755*, 2025. 3

Hao Gao, Shaoyu Chen, Bo Jiang, Bencheng Liao, Yiang Shi, Xiaoyang Guo, Yuechuan Pu, Haoran Yin, Xiangyu Li, Xinbang Zhang, et al. Rad: Training an end-to-end driving policy via large-scale 3dgs-based reinforcement learning. *arXiv preprint arXiv:2502.13144*, 2025. 3

Junru Gu, Chenxu Hu, Tianyuan Zhang, Xuanyao Chen, Yilun Wang, Yue Wang, and Hang Zhao. Vip3d: End-to-end visual trajectory prediction via 3d agent queries. In *Proceedings of the IEEE/CVF Conference on Computer Vision and Pattern Recognition*, pp. 5496–5506, 2023. 1

Daya Guo, Dejian Yang, Haowei Zhang, Junxiao Song, Ruoyu Zhang, Runxin Xu, Qihao Zhu, Shirong Ma, Peiyi Wang, Xiao Bi, et al. Deepseek-r1: Incentivizing reasoning capability in llms via reinforcement learning. *arXiv preprint arXiv:2501.12948*, 2025. 3

Danijar Hafner, Jurgis Pasukonis, Jimmy Ba, and Timothy Lillicrap. Mastering diverse domains through world models. *arXiv preprint arXiv:2301.04104*, 2023. 3

Deepti Hegde, Rajeev Yasarla, Hong Cai, Shizhong Han, Apratim Bhattacharyya, Shweta Mahajan, Litian Liu, Risheek Garrepalli, Vishal M Patel, and Fatih Porikli. Distilling multi-modal large language models for autonomous driving. In *Proceedings of the Computer Vision and Pattern Recognition Conference*, pp. 27575–27585, 2025. 3, 21

Jonathan Ho, Ajay Jain, and Pieter Abbeel. Denoising diffusion probabilistic models. *Advances in neural information processing systems*, 33:6840–6851, 2020. 4, 24

Shengchao Hu, Li Chen, Penghao Wu, Hongyang Li, Junchi Yan, and Dacheng Tao. St-p3: End-to-end vision-based autonomous driving via spatial-temporal feature learning. In *European Conference on Computer Vision*, pp. 533–549. Springer, 2022. 1

Yihan Hu, Jiazhi Yang, Li Chen, Keyu Li, Chonghao Sima, Xizhou Zhu, Siqi Chai, Senyao Du, Tianwei Lin, Wenhai Wang, et al. Planning-oriented autonomous driving. In *Proceedings of the IEEE/CVF conference on computer vision and pattern recognition*, pp. 17853–17862, 2023. 1, 4, 8, 21

Zhiyu Huang, Xinshuo Weng, Maximilian Igl, Yuxiao Chen, Yulong Cao, Boris Ivanovic, Marco Pavone, and Chen Lv. Gen-drive: Enhancing diffusion generative driving policies with reward modeling and reinforcement learning fine-tuning. In *2025 IEEE International Conference on Robotics and Automation (ICRA)*, pp. 3445–3451. IEEE, 2025. 3

Aaron Hurst, Adam Lerer, Adam P Goucher, Adam Perelman, Aditya Ramesh, Aidan Clark, AJ Ostrow, Akila Welihinda, Alan Hayes, Alec Radford, et al. Gpt-4o system card. *arXiv preprint arXiv:2410.21276*, 2024. 20

Jyh-Jing Hwang, Runsheng Xu, Hubert Lin, Wei-Chih Hung, Jingwei Ji, Kristy Choi, Di Huang, Tong He, Paul Covington, Benjamin Sapp, et al. Emma: End-to-end multimodal model for autonomous driving. *arXiv preprint arXiv:2410.23262*, 2024. 1, 2, 3, 4, 18

Xiaosong Jia, Yulu Gao, Li Chen, Junchi Yan, Patrick Langechuan Liu, and Hongyang Li. Driveadapter: Breaking the coupling barrier of perception and planning in end-to-end autonomous driving. In *Proceedings of the IEEE/CVF International Conference on Computer Vision*, pp. 7953–7963, 2023a. 8

Xiaosong Jia, Penghao Wu, Li Chen, Jiangwei Xie, Conghui He, Junchi Yan, and Hongyang Li. Think twice before driving: Towards scalable decoders for end-to-end autonomous driving. In *Proceedings of the IEEE/CVF Conference on Computer Vision and Pattern Recognition*, pp. 21983–21994, 2023b. 8

Xiaosong Jia, Zhenjie Yang, Qifeng Li, Zhiyuan Zhang, and Junchi Yan. Bench2drive: Towards multi-ability benchmarking of closed-loop end-to-end autonomous driving. *Advances in Neural Information Processing Systems*, 37:819–844, 2024. 8

Xiaosong Jia, Junqi You, Zhiyuan Zhang, and Junchi Yan. Drivetransformer: Unified transformer for scalable end-to-end autonomous driving. *arXiv preprint arXiv:2503.07656*, 2025. 8

Bo Jiang, Shaoyu Chen, Qing Xu, Bencheng Liao, Jiajie Chen, Helong Zhou, Qian Zhang, Wenyu Liu, Chang Huang, and Xinggang Wang. Vad: Vectorized scene representation for efficient autonomous driving. In *Proceedings of the IEEE/CVF International Conference on Computer Vision*, pp. 8340–8350, 2023. 1, 4, 8, 21

Bo Jiang, Shaoyu Chen, Bencheng Liao, Xingyu Zhang, Wei Yin, Qian Zhang, Chang Huang, Wenyu Liu, and Xinggang Wang. Senna: Bridging large vision-language models and end-to-end autonomous driving. *arXiv preprint arXiv:2410.22313*, 2024a. 1, 3, 22, 25

Bo Jiang, Shaoyu Chen, Qian Zhang, Wenyu Liu, and Xinggang Wang. Alphadrive: Unleashing the power of vlms in autonomous driving via reinforcement learning and reasoning. *arXiv preprint arXiv:2503.07608*, 2025. 3

Xiaohui Jiang, Shuailin Li, Yingfei Liu, Shihao Wang, Fan Jia, Tiancai Wang, Lijin Han, and Xiangyu Zhang. Far3d: Expanding the horizon for surround-view 3d object detection. In *Proceedings of the AAAI Conference on Artificial Intelligence*, volume 38, pp. 2561–2569, 2024b. 1

Jinkyu Kim, Anna Rohrbach, Trevor Darrell, John Canny, and Zeynep Akata. Textual explanations for self-driving vehicles. In *Proceedings of the European conference on computer vision (ECCV)*, pp. 563–578, 2018. 22

Derun Li, Jianwei Ren, Yue Wang, Xin Wen, Pengxiang Li, Leimeng Xu, Kun Zhan, Zhongpu Xia, Peng Jia, Xianpeng Lang, et al. Finetuning generative trajectory model with reinforcement learning from human feedback. *arXiv preprint arXiv:2503.10434*, 2025a. 3, 7

Yingyan Li, Yuqi Wang, Yang Liu, Jiawei He, Lue Fan, and Zhaoxiang Zhang. End-to-end driving with online trajectory evaluation via bev world model. *arXiv preprint arXiv:2504.01941*, 2025b. 8, 9

Yue Li, Meng Tian, Dechang Zhu, Jiangtong Zhu, Zhenyu Lin, Zhiwei Xiong, and Xinhai Zhao. Drive-r1: Bridging reasoning and planning in vlms for autonomous driving with reinforcement learning. *arXiv preprint arXiv:2506.18234*, 2025c. 3, 7

Zhenxin Li, Kailin Li, Shihao Wang, Shiyi Lan, Zhiding Yu, Yishen Ji, Zhiqi Li, Ziyue Zhu, Jan Kautz, Zuxuan Wu, et al. Hydra-mdp: End-to-end multimodal planning with multi-target hydra-distillation. *arXiv preprint arXiv:2406.06978*, 2024. 8, 19

Bencheng Liao, Shaoyu Chen, Haoran Yin, Bo Jiang, Cheng Wang, Sixu Yan, Xinbang Zhang, Xiangyu Li, Ying Zhang, Qian Zhang, et al. Diffusiondrive: Truncated diffusion model for end-to-end autonomous driving. *arXiv preprint arXiv:2411.15139*, 2024. 1, 3, 4, 8, 9

Haochen Liu, Tianyu Li, Haohan Yang, Li Chen, Caojun Wang, Ke Guo, Haochen Tian, Hongchen Li, Hongyang Li, and Chen Lv. Reinforced refinement with self-aware expansion for end-to-end autonomous driving. *arXiv preprint arXiv:2506.09800*, 2025. 3

Haotian Liu, Chunyuan Li, Qingyang Wu, and Yong Jae Lee. Visual instruction tuning, 2023a. 25

Haotian Liu, Chunyuan Li, Qingyang Wu, and Yong Jae Lee. Visual instruction tuning. *Advances in neural information processing systems*, 36:34892–34916, 2023b. 20

Haotian Liu, Chunyuan Li, Yuheng Li, Bo Li, Yuanhan Zhang, Sheng Shen, and Yong Jae Lee. Llava-next: Improved reasoning, ocr, and world knowledge, January 2024a. URL https://llava-vl.github.io/blog/2024-01-30-llava-next/. 20

Songming Liu, Lingxuan Wu, Bangguo Li, Hengkai Tan, Huayu Chen, Zhengyi Wang, Ke Xu, Hang Su, and Jun Zhu. Rdt-1b: a diffusion foundation model for bimanual manipulation. *arXiv preprint arXiv:2410.07864*, 2024b. 3

Zuyan Liu, Yuhao Dong, Ziwei Liu, Winston Hu, Jiwen Lu, and Yongming Rao. Oryx mllm: On-demand spatial-temporal understanding at arbitrary resolution. *arXiv preprint arXiv:2409.12961*, 2024c. 20

Yingzi Ma, Yulong Cao, Jiachen Sun, Marco Pavone, and Chaowei Xiao. Dolphins: Multimodal language model for driving. In *European Conference on Computer Vision*, pp. 403–420. Springer, 2024. 20

Srikanth Malla, Chiho Choi, Isht Dwivedi, Joon Hee Choi, and Jiachen Li. Drama: Joint risk localization and captioning in driving. In *Proceedings of the IEEE/CVF winter conference on applications of computer vision*, pp. 1043–1052, 2023. 22, 25

Jiageng Mao, Yuxi Qian, Junjie Ye, Hang Zhao, and Yue Wang. Gpt-driver: Learning to drive with gpt. *arXiv preprint arXiv:2310.01415*, 2023a. 2, 3, 4

Jiageng Mao, Junjie Ye, Yuxi Qian, Marco Pavone, and Yue Wang. A language agent for autonomous driving. *arXiv preprint arXiv:2311.10813*, 2023b. 2, 3

Ana-Maria Marcu, Long Chen, Jan Hünermann, Alice Karnsund, Benoit Hanotte, Prajwal Chidananda, Saurabh Nair, Vijay Badrinarayanan, Alex Kendall, Jamie Shotton, et al. Lingoqa: Visual question answering for autonomous driving. In *European Conference on Computer Vision*, pp. 252–269. Springer, 2024. 8, 22, 25

Alexander Quinn Nichol and Prafulla Dhariwal. Improved denoising diffusion probabilistic models. In *International conference on machine learning*, pp. 8162–8171. PMLR, 2021. 4, 20

Takayuki Osa, Joni Pajarinen, Gerhard Neumann, J Andrew Bagnell, Pieter Abbeel, Jan Peters, et al. An algorithmic perspective on imitation learning. *Foundations and Trends® in Robotics*, 7(1-2): 1–179, 2018. 6

Chenbin Pan, Burhaneddin Yaman, Tommaso Nesti, Abhirup Mallik, Alessandro G Allievi, Senem Velipasalar, and Liu Ren. Vlp: Vision language planning for autonomous driving. In *Proceedings of the IEEE/CVF Conference on Computer Vision and Pattern Recognition*, pp. 14760–14769, 2024. 3, 21

William Peebles and Saining Xie. Scalable diffusion models with transformers. In *Proceedings of the IEEE/CVF international conference on computer vision*, pp. 4195–4205, 2023. 5, 24

Jonah Philion and Sanja Fidler. Lift, splat, shoot: Encoding images from arbitrary camera rigs by implicitly unprojecting to 3d. In *Computer Vision–ECCV 2020: 16th European Conference, Glasgow, UK, August 23–28, 2020, Proceedings, Part XIV 16*, pp. 194–210. Springer, 2020. 1

Dustin Podell, Zion English, Kyle Lacey, Andreas Blattmann, Tim Dockhorn, Jonas Müller, Joe Penna, and Robin Rombach. Sdxl: Improving latent diffusion models for high-resolution image synthesis. *arXiv preprint arXiv:2307.01952*, 2023. 3

Tianwen Qian, Jingjing Chen, Linhai Zhuo, Yang Jiao, and Yu-Gang Jiang. Nuscenes-qa: A multi-modal visual question answering benchmark for autonomous driving scenario. In *Proceedings of the AAAI Conference on Artificial Intelligence*, volume 38, pp. 4542–4550, 2024. 22, 25

Allen Z Ren, Justin Lidard, Lars L Ankile, Anthony Simeonov, Pulkit Agrawal, Anirudha Majumdar, Benjamin Burchfiel, Hongkai Dai, and Max Simchowitz. Diffusion policy policy optimization. *arXiv preprint arXiv:2409.00588*, 2024. 3, 6, 10, 20

Hao Shao, Yuxuan Hu, Letian Wang, Guanglu Song, Steven L Waslander, Yu Liu, and Hongsheng Li. Lmdrive: Closed-loop end-to-end driving with large language models. In *Proceedings of the IEEE/CVF Conference on Computer Vision and Pattern Recognition*, pp. 15120–15130, 2024a. 3

Zhihong Shao, Peiyi Wang, Qihao Zhu, Runxin Xu, Junxiao Song, Xiao Bi, Haowei Zhang, Mingchuan Zhang, YK Li, Y Wu, et al. Deepseekmath: Pushing the limits of mathematical reasoning in open language models. *arXiv preprint arXiv:2402.03300*, 2024b. 6, 7

Noam Shazeer. Glu variants improve transformer. *arXiv preprint arXiv:2002.05202*, 2020. 5

Chonghao Sima, Katrin Renz, Kashyap Chitta, Li Chen, Hanxue Zhang, Chengen Xie, Jens Beißwenger, Ping Luo, Andreas Geiger, and Hongyang Li. Drivelm: Driving with graph visual question answering. In *European Conference on Computer Vision*, pp. 256–274. Springer, 2024. 8, 20, 22, 23, 25

Jianlin Su, Murtadha Ahmed, Yu Lu, Shengfeng Pan, Wen Bo, and Yunfeng Liu. Roformer: Enhanced transformer with rotary position embedding. *Neurocomputing*, 568:127063, 2024. 5

Xiaoyu Tian, Junru Gu, Bailin Li, Yicheng Liu, Yang Wang, Zhiyong Zhao, Kun Zhan, Peng Jia, Xianpeng Lang, and Hang Zhao. Drivevlm: The convergence of autonomous driving and large vision-language models. *arXiv preprint arXiv:2402.12289*, 2024. 1, 3, 21

Peng Wang, Shuai Bai, Sinan Tan, Shijie Wang, Zhihao Fan, Jinze Bai, Keqin Chen, Xuejing Liu, Jialin Wang, Wenbin Ge, Yang Fan, Kai Dang, Mengfei Du, Xuancheng Ren, Rui Men, Dayiheng Liu, Chang Zhou, Jingren Zhou, and Junyang Lin. Qwen2-vl: Enhancing vision-language model's perception of the world at any resolution. *arXiv preprint arXiv:2409.12191*, 2024a. 20

Shihao Wang, Zhiding Yu, Xiaohui Jiang, Shiyi Lan, Min Shi, Nadine Chang, Jan Kautz, Ying Li, and Jose M Alvarez. Omnidrive: A holistic llm-agent framework for autonomous driving with 3d perception, reasoning and planning. *arXiv preprint arXiv:2405.01533*, 2024b. 2, 3, 18, 22, 23, 25

Jason Wei, Xuezhi Wang, Dale Schuurmans, Maarten Bosma, Fei Xia, Ed Chi, Quoc V Le, Denny Zhou, et al. Chain-of-thought prompting elicits reasoning in large language models. *Advances in neural information processing systems*, 35:24824–24837, 2022. 2, 3

Xinshuo Weng, Boris Ivanovic, Yan Wang, Yue Wang, and Marco Pavone. Para-drive: Parallelized architecture for real-time autonomous driving. In *Proceedings of the IEEE/CVF Conference on Computer Vision and Pattern Recognition*, pp. 15449–15458, 2024. 8, 9

Ronald J Williams. Simple statistical gradient-following algorithms for connectionist reinforcement learning. *Machine learning*, 8:229–256, 1992. 7, 10

Penghao Wu, Xiaosong Jia, Li Chen, Junchi Yan, Hongyang Li, and Yu Qiao. Trajectory-guided control prediction for end-to-end autonomous driving: A simple yet strong baseline. *Advances in Neural Information Processing Systems*, 35:6119–6132, 2022. 8

Shuo Xing, Chengyuan Qian, Yuping Wang, Hongyuan Hua, Kexin Tian, Yang Zhou, and Zhengzhong Tu. Openemma: Open-source multimodal model for end-to-end autonomous driving. *arXiv preprint arXiv:2412.15208*, 2024. 2, 3

Zebin Xing, Xingyu Zhang, Yang Hu, Bo Jiang, Tong He, Qian Zhang, Xiaoxiao Long, and Wei Yin. Goalflow: Goal-driven flow matching for multimodal trajectories generation in end-to-end autonomous driving. In *Proceedings of the Computer Vision and Pattern Recognition Conference*, pp. 1602–1611, 2025. 3

Li Xu, He Huang, and Jun Liu. Sutd-trafficqa: A question answering benchmark and an efficient network for video reasoning over traffic events. In *Proceedings of the IEEE/CVF conference on computer vision and pattern recognition*, pp. 9878–9888, 2021. 22, 25

Zhenhua Xu, Yujia Zhang, Enze Xie, Zhen Zhao, Yong Guo, Kwan-Yee K Wong, Zhenguo Li, and Hengshuang Zhao. Drivegpt4: Interpretable end-to-end autonomous driving via large language model. *IEEE Robotics and Automation Letters*, 2024. 22, 25

Sixu Yan, Zeyu Zhang, Muzhi Han, Zaijin Wang, Qi Xie, Zhitian Li, Zhehan Li, Hangxin Liu, Xinggang Wang, and Song-Chun Zhu. M 2 diffuser: Diffusion-based trajectory optimization for mobile manipulation in 3d scenes. *IEEE Transactions on Pattern Analysis and Machine Intelligence*, 2025. 3

Brian Yang, Huangyuan Su, Nikolaos Gkanatsios, Tsung-Wei Ke, Ayush Jain, Jeff Schneider, and Katerina Fragkiadaki. Diffusion-es: Gradient-free planning with diffusion for autonomous and instruction-guided driving. In *Proceedings of the IEEE/CVF Conference on Computer Vision and Pattern Recognition*, pp. 15342–15353, 2024. 3

Jingfeng Yao, Bin Yang, and Xinggang Wang. Reconstruction vs. generation: Taming optimization dilemma in latent diffusion models. In *Proceedings of the IEEE/CVF Conference on Computer Vision and Pattern Recognition*, 2025. 5

Chengran Yuan, Zhanqi Zhang, Jiawei Sun, Shuo Sun, Zefan Huang, Christina Dao Wen Lee, Dongen Li, Yuhang Han, Anthony Wong, Keng Peng Tee, et al. Drama: An efficient end-to-end motion planner for autonomous driving with mamba. *arXiv preprint arXiv:2408.03601*, 2024. 8

Kai Zeng, Zhanqian Wu, Kaixin Xiong, Xiaobao Wei, Xiangyu Guo, Zhenxin Zhu, Kalok Ho, Lijun Zhou, Bohan Zeng, Ming Lu, et al. Rethinking driving world model as synthetic data generator for perception tasks. *arXiv preprint arXiv:2510.19195*, 2025. 3

Jiang-Tian Zhai, Ze Feng, Jinhao Du, Yongqiang Mao, Jiang-Jiang Liu, Zichang Tan, Yifu Zhang, Xiaoqing Ye, and Jingdong Wang. Rethinking the open-loop evaluation of end-to-end autonomous driving in nuscenes. *arXiv preprint arXiv:2305.10430*, 2023. 8

Biao Zhang and Rico Sennrich. Root mean square layer normalization. *Advances in neural information processing systems*, 32, 2019. 6

Diankun Zhang, Zhijie Zheng, Haoyu Niu, Xueqing Wang, and Xiaojun Liu. Fully sparse transformer 3-d detector for lidar point cloud. *IEEE Transactions on Geoscience and Remote Sensing*, 61:1–12, 2023. 1

Diankun Zhang, Guoan Wang, Runwen Zhu, Jianbo Zhao, Xiwu Chen, Siyu Zhang, Jiahao Gong, Qibin Zhou, Wenyuan Zhang, Ningzi Wang, et al. Sparsead: Sparse query-centric paradigm for efficient end-to-end autonomous driving. *arXiv preprint arXiv:2404.06892*, 2024a. 1

Dongkun Zhang, Jiaming Liang, Ke Guo, Sha Lu, Qi Wang, Rong Xiong, Zhenwei Miao, and Yue Wang. Carplanner: Consistent auto-regressive trajectory planning for large-scale reinforcement learning in autonomous driving. *arXiv preprint arXiv:2502.19908*, 2025. 3

Ruijun Zhang, Xianda Guo, Wenzhao Zheng, Chenming Zhang, Kurt Keutzer, and Long Chen. Instruct large language models to drive like humans. *arXiv preprint arXiv:2406.07296*, 2024b. 4

Songyan Zhang, Wenhui Huang, Zihui Gao, Hao Chen, and Chen Lv. Wisead: Knowledge augmented end-to-end autonomous driving with vision-language model. *arXiv preprint arXiv:2412.09951*, 2024c. 2, 3

Rui Zhao, Qirui Yuan, Jinyu Li, Haofeng Hu, Yun Li, Chengyuan Zheng, and Fei Gao. Sce2drivex: A generalized mllm framework for scene-to-drive learning. *arXiv preprint arXiv:2502.14917*, 2025. 2, 3

Yinan Zheng, Ruiming Liang, Kexin Zheng, Jinliang Zheng, Liyuan Mao, Jianxiong Li, Weihao Gu, Rui Ai, Shengbo Eben Li, Xianyuan Zhan, et al. Diffusion-based planning for autonomous driving with flexible guidance. *arXiv preprint arXiv:2501.15564*, 2025. 3

Zangwei Zheng, Xiangyu Peng, Tianji Yang, Chenhui Shen, Shenggui Li, Hongxin Liu, Yukun Zhou, Tianyi Li, and Yang You. Open-sora: Democratizing efficient video production for all. *arXiv preprint arXiv:2412.20404*, 2024. 3

Ziyuan Zhong, Davis Rempe, Danfei Xu, Yuxiao Chen, Sushant Veer, Tong Che, Baishakhi Ray, and Marco Pavone. Guided conditional diffusion for controllable traffic simulation. In *2023 IEEE international conference on robotics and automation (ICRA)*, pp. 3560–3566. IEEE, 2023. 3

Xin Zhou, Dingkang Liang, Sifan Tu, Xiwu Chen, Yikang Ding, Dingyuan Zhang, Feiyang Tan, Hengshuang Zhao, and Xiang Bai. Hermes: A unified self-driving world model for simultaneous 3d scene understanding and generation. In *Proceedings of the IEEE/CVF International Conference on Computer Vision*, pp. 27817–27827, 2025a. 3

Zewei Zhou, Tianhui Cai, Yun Zhao, Seth Z.and Zhang, Zhiyu Huang, Bolei Zhou, and Jiaqi Ma. Autovla: A vision-language-action model for end-to-end autonomous driving with adaptive reasoning and reinforcement fine-tuning. *arXiv preprint arXiv:2506.13757*, 2025b. 8, 21

Jinguo Zhu, Weiyun Wang, Zhe Chen, Zhaoyang Liu, Shenglong Ye, Lixin Gu, Yuchen Duan, Hao Tian, Weijie Su, Jie Shao, et al. Internvl3: Exploring advanced training and test-time recipes for open-source multimodal models. *arXiv preprint arXiv:2504.10479*, 2025. 5, 8, 9, 23, 24

A APPENDIX

We organize the supplementary material as follows. First, in Appx. B, we address potential questions that may arise from reading the main text. We then report ReCogDrive's performance on the NAVSIM and DriveBench benchmarks, along with more detailed ablation studies in Appx. C. In Appx. D, we provide details of the training data collection and processing pipeline. Appx. E describes ReCogDrive's training and inference implementation, including all key hyperparameters, and also provides details of the evaluation metrics used on NAVSIM and Bench2Drive. Appx. F and Appx. H discuss the limitations of the method and the broader impacts. We also provide our LLM Usage Statement in Appx. G. Finally, Appx. I presents additional qualitative results, including extensive visualizations on NAVSIM and Bench2Drive, comparisons between IL and RL trajectories, driving dialogues, and analyses of failure cases.

B QUESTIONS

Q1. *What is the technical novelty in this paper?*

The key novelty of this work is a reinforced cognitive framework for autonomous driving that integrates a VLM with a diffusion-based planner. Unlike prior driving VLA approaches (e.g., EMMA (Hwang et al., 2024), OmniDrive (Wang et al., 2024b)) that generate trajectories purely in the text space, our framework injects VLM-derived driving priors into a diffusion planner, avoiding slow inference, infeasible actions, and trajectory errors. Within this unified framework, we further contribute three innovations: (i) a scalable hierarchical data pipeline that mimics the sequential cognitive process of human drivers through generation, refinement, and quality control, enabling flexible adaptation of VLMs to diverse driving scenarios; (ii) a cognition-guided diffusion planner that leverages VLM-derived priors to efficiently generate continuous and stable trajectories, surpassing plain-text and Transfuser-like (Chitta et al., 2022) decoders; and (iii) Diffusion Group Relative Policy Optimization (DiffGRPO), a reinforcement learning scheme tailored for diffusion-based planners in autonomous driving VLAs, enabling simulation-driven policy optimization for safer and more comfortable driving.

Q2. *Does the VLM merely act as a feature extractor?*

ReCogDrive consists of a Vision-Language Model and a diffusion planner. In our framework, the VLM can produce high-level instructions or chain-of-thought reasoning to guide planning. However, as shown in Tab. 11, reinforcement learning alone already achieves state-of-the-art performance on the NAVSIM benchmark. Incorporating CoT-based guidance provides no gain, mainly due to the limited diversity of NAVSIM scenarios. Moreover, Bench2Drive already supplies explicit navigation instructions. For efficiency, we therefore keep VLM-based textual guidance optional.

Q3. *Why was the model trained on datasets such as CODA-LM and OmniDrive, yet not evaluated on them?*

Our model is trained on a mixture of 12 open-source driving datasets, which enables handling multiple scenes and tasks. We observed that most existing benchmarks, including CODA-LM and OmniDrive, employ traditional metrics such as BLEU and ROUGE. These metrics evaluate performance by calculating the textual similarity between a model's response and the ground-truth answer. Such metrics primarily assess dataset-specific fitting rather than general reasoning ability. Therefore, to better evaluate the model's true Visual Question Answering (VQA) capabilities, we utilize the GPT-Score from the DriveLM and DriveBench benchmarks, as presented in Tab. 5.

Q4. *Does DriveVQA accurately reflect the capabilities of a VLM for autonomous driving?*

DriveBench has shown that many VLMs' decision accuracy does not degrade with visual quality, indicating a reliance on priors rather than genuine visual understanding. Therefore, we primarily use the Planning task to evaluate a model's practical capabilities in dynamic driving scenarios. However, for completeness and to facilitate comparison with existing work, we also provide the VQA results on the DriveLM and DriveBench benchmarks.

Q5. *Does ReCogDrive rely on high-quality QA annotations to generalize to other domains?*

ReCogDrive achieves state-of-the-art results by leveraging high-quality driving QA datasets. However, a key contribution of our work is the scalable hierarchical data generation pipeline. Built on advanced VLMs deployed with Sglang, this pipeline can automatically generate large-scale QA annotations, followed by normalization, scoring, and filtering to ensure quality. This design ensures efficiency and adaptability, enabling transfer to new domains without costly manual annotation.

Q6. *Why does applying the formula in Eq. 14 to the averaged sub-metrics in Tab. 1 not yield the reported PDM Score?*

As documented in a NAVSIM issue [1], the PDMS score is calculated per scene using the formula and is then averaged across all scenes. Applying the formula to sub-metrics that have already been averaged is a different computation and will thus lead to a different final value.

Q7. *Why does the paper adopt such a low discount factor (0.6) for a long-horizon driving task?*

In Eq. 12, the discount factor is applied across denoising steps rather than over the temporal horizon of the driving task. In diffusion-based planning, early denoising steps amplify high-variance noise and often destabilize learning. A smaller discount factor places greater weight on later, more reliable denoising steps, which directly improves stability and feasibility of generated trajectories. This design choice is thus motivated by the dynamics of the denoising process rather than by a short-horizon assumption of the driving task itself.

Q8. *Why does the paper employ a BC loss instead of the standard KL-divergence loss?*

We employ a BC-style objective as a stable surrogate for KL regularization. Direct KL constraints often lead to unstable optimization in diffusion-based RL, since variance amplification across denoising steps can cause noisy and unreliable gradients. In contrast, the BC formulation provides smoother updates and better training stability, which proved crucial for policy learning effectiveness.

Q9. *Does the diffusion planner only provide performance gains?*

As shown in Tab. 4, beyond the $+2.4$ PDMS improvement over plain-text VLM outputs, the diffusion planner also achieves $3.5\times$ faster inference by requiring only a forward pass rather than autoregressive generation. More importantly, it eliminates the 0.01% template mismatch errors observed in plain-text decoding, an unacceptable rate in safety-critical driving, making it both more accurate and more reliable for practical autonomous driving.

C More Results

Table 7: **Performance comparison on Navtest Benchmark with extended metrics.**

Method	NC↑	DAC↑	EP↑	TTC↑	C↑	TL↑	DDC↑	LK↑	EC↑	EPDMS↑
Transfuser (Chitta et al., 2022)	97.7	92.8	79.2	92.8	**100**	99.9	98.3	67.6	95.3	77.8
VADv2 (Chen et al., 2024b)	97.3	91.7	77.6	92.7	**100**	99.9	98.2	66.0	97.4	76.6
Hydra-MDP (Li et al., 2024)	97.5	96.3	80.1	93.0	**100**	99.9	98.3	65.5	97.4	79.8
Hydra-MDP++ (Li et al., 2024)	97.9	**96.5**	79.2	93.4	**100**	**100**	98.9	67.2	**97.7**	80.6
ARTEMIS (Feng et al., 2025)	98.3	95.1	81.5	97.4	**100**	99.8	98.6	**96.5**	98.3	83.1
ReCogDrive	**98.3**	95.9	**87.7**	**97.7**	97.9	97.4	**99.3**	86.0	81.9	**84.2**

Experiments on NAVSIM with extended metrics. Hydra MDP++ (Li et al., 2024) introduces additional evaluation metrics: Traffic Light Compliance (TL), Lane Keeping Ability (LK), Driving Direction Compliance (DDC) and Extended Comfort (EC) to more comprehensively assess driving performance. We evaluate ReCogDrive on NAVSIM using these extended metrics as well. Tab. 7

[1] https://github.com/autonomousvision/navsim/issues/116

Table 8: **Evaluation of ReCogDrive-VLM on DriveBench.** We report ReCogDrive-VLM's performance across four key driving dimensions: perception, prediction, planning, and behavior. Results are shown under three input settings: Clean (unaltered images), Corr. (images with averaged corruptions), and T.O. (text-only inputs).

Method	Size	Type	Perception			Prediction			Planning			Behavior		
			Clean	Corr.	T.O.	Clean	Corr.	T.O.	Clean	Corr.	T.O.	Clean	Corr.	T.O.
Human	-	-	47.67	38.32	-	-	-	-	-	-	-	69.51	54.09	-
GPT-4o (Hurst et al., 2024)	-	Commercial	35.37	35.25	36.48	51.30	49.94	49.05	75.75	75.36	73.21	45.40	44.33	50.03
LLaVA-1.5 (Liu et al., 2023b)	7 B	Open	23.22	22.95	22.31	22.02	17.54	14.64	29.15	31.51	32.45	13.60	13.62	14.91
LLaVA-1.5 (Liu et al., 2023b)	13 B	Open	23.35	23.37	22.37	36.98	37.78	23.98	34.26	34.99	38.85	32.99	32.43	32.79
LLaVA-NeXT (Liu et al., 2024a)	7 B	Open	24.15	19.62	13.86	35.07	35.89	28.36	45.27	44.36	27.58	48.16	39.44	11.92
InternVL2 (Chen et al., 2024d)	8 B	Open	32.36	32.68	33.60	45.52	37.93	48.89	53.27	55.25	34.56	**54.58**	40.78	20.14
Phi-3 (Abdin et al., 2024)	4.2 B	Open	22.88	23.93	28.26	40.11	37.27	22.61	60.03	61.31	46.88	45.20	44.57	28.22
Phi-3.5 (Abdin et al., 2024)	4.2 B	Open	27.52	27.51	28.26	45.13	38.21	4.92	31.91	28.36	46.30	37.89	49.13	39.16
Oryx (Liu et al., 2024c)	7 B	Open	17.02	15.97	18.47	48.13	46.63	12.77	53.57	55.76	48.26	33.92	33.81	23.94
Qwen2-VL (Wang et al., 2024a)	7 B	Open	28.99	27.85	35.16	37.89	39.55	37.77	57.04	54.78	41.66	49.07	47.68	**54.48**
Qwen2-VL (Wang et al., 2024a)	72 B	Open	30.13	26.92	17.70	**49.35**	43.49	5.57	61.30	63.07	53.35	51.26	**49.78**	39.46
DriveLM (Sima et al., 2024)	7 B	Specialist	16.85	16.00	8.75	44.33	39.71	4.70	68.71	67.60	65.24	42.78	40.37	27.83
Dolphins (Ma et al., 2024)	7 B	Specialist	9.59	10.84	11.01	32.66	29.88	39.98	52.91	53.77	60.98	8.81	8.25	11.92
ReCogDrive-VLM	8 B	Specialist	**64.95**	**63.35**	**71.44**	49.34	**48.92**	**53.49**	**70.20**	**72.5**	**71.76**	42.36	42.76	44.00

Table 9: Impact of Different BC Loss Weights λ.

BC Wt.	NC	DAC	TTC	Conf.	EP	PDMS
0.001	97.9	97.3	94.9	100	87.3	90.8
0.01	97.9	97.5	94.9	100	86.0	90.3
0.1	97.6	97.2	93.9	100	85.0	89.3

Table 10: Impact of Different Min Samplings $\sigma_{\text{min}}^{\text{exp}}$.

Min Samp.	NC	DAC	TTC	Conf.	EP	PDMS
0.01	98.2	97.8	95.6	100	82.8	89.5
0.02	97.9	97.3	94.9	100	87.3	90.8
0.04	97.9	97.7	95.3	100	85.7	90.5

Table 11: Comparison between trajectory-only (Only Traj), adding high-level command (w/ High Com.), and chain-of-thought (w/ CoT).

Mode	NC	DAC	TTC	Conf.	EP	PDMS
Only Traj	97.9	97.3	94.9	100	87.3	90.8
w/ High Com.	97.9	97.3	94.9	100	87.2	90.8
w/ CoT	97.8	97.2	94.8	100	87.1	90.7

Table 12: Impact of different discount factors γ. We use discounting to reduce the influence of early-step noise during the diffusion process.

Discount	NC	DAC	TTC	Conf.	EP	PDMS
0.6	97.9	97.3	94.9	100	87.3	90.8
0.8	98.0	97.6	95.3	100	85.9	90.5
1.0	97.9	97.5	94.9	100	86.0	90.3

compares our approach against existing methods under this metrics. ReCogDrive achieves state of the art scores in Driving Direction Compliance (DDC), No at-fault Collisions (NC), Ego Progress (EP) and Time to Collision (TTC), and delivers a 1.1 improvement in EPDMS over ARTEMIS (Feng et al., 2025), demonstrating the effectiveness of our method.

Evaluations of VLMs across driving tasks. Tab. 8 reports results on *DriveBench* across perception, prediction, planning, and behavior. ReCogDrive-VLM achieves the best overall performance and shows strong robustness under both corrupted and text-only settings, outperforming general-purpose VLMs (e.g., Qwen2-VL, InternVL2) and specialist models (e.g., DriveLM, Dolphins). These results demonstrate the strong driving scene understanding capability of our ReCogDrive-VLM.

Impact of Different Behavior Clone Loss Weights. Tab. 9 examines the impact of the BC loss weight λ. As λ decreases, the policy learns more aggressively, and at $\lambda = 0.001$ ego progress increases to 87.3 with slight declines in NC, DAC, and TTC, yielding the highest PDMS.

Impact of Different Min Sampling Values. Following (Ren et al., 2024; Nichol & Dhariwal, 2021), we apply a cosine schedule to the diffusion noise variances σ_k and clip them to a minimum value $\sigma_{\text{min}}^{\text{exp}}$. Clipping σ_k to a nonzero minimum encourages the diffusion policy to sample more diverse trajectories, yet overly large $\sigma_{\text{min}}^{\text{exp}}$ can destabilize training. Setting $\sigma_{\text{min}}^{\text{exp}} = 0.02$ achieves a PDMS of 90.8, as shown in Tab. 10.

Effect of VLM guidance modes. As shown in Tab. 11, outputting only trajectory achieves performance comparable to adding high-level command guidance, with almost identical PDMS scores. Interestingly, incorporating chain-of-thought reasoning does not further improve the results; instead, it slightly decreases the PDMS score by 0.1. This suggests that the current NAVSIM benchmark

Table 13: **Planning performance on the nuScenes val set.** We train our model on Bench2Drive, and report both zero-shot transfer results on nuScenes and performance after fine-tuning on nuScenes.

Method	L2 (m)↓				Collision (%)↓			
	1s	2s	3s	Avg.	1s	2s	3s	Avg.
UniAD (Hu et al., 2023)	0.20	0.42	0.75	0.46	0.02	0.25	0.84	0.37
VLP (Pan et al., 2024)	0.30	0.53	0.84	0.55	0.01	0.07	0.38	0.15
VAD (Jiang et al., 2023)	0.17	0.34	0.60	0.37	0.07	0.10	0.24	0.14
DriveVLM (Tian et al., 2024)	0.18	0.34	0.68	0.40	0.10	0.22	0.45	0.27
DiMA-Dual+ (Hegde et al., 2025)	0.14	0.27	0.46	0.29	0.05	0.07	0.15	0.09
AutoVLA (Zhou et al., 2025b)	0.22	0.39	0.61	0.41	0.10	0.17	0.28	0.18
ReCogDrive (zero-shot)	1.34	1.91	2.69	1.98	0.07	0.57	0.82	0.82
ReCogDrive (fine-tune)	0.17	0.34	0.63	0.38	0.07	0.09	0.16	0.10

Table 14: Sensitivity of PDMS to the EP weight w_{EP} (fixed $w_{\text{TTC}} = 5.0$, $w_{\text{C}} = 2.0$).

w_{EP}	NC	DAC	TTC	Conf.	EP	PDMS
5.0	98.6	97.8	96.2	100	84.0	90.3
10.0	97.9	97.3	94.9	100	87.3	90.8
20.0	97.8	97.3	94.2	100	87.3	90.5
30.0	97.6	97.2	93.1	99.6	87.6	90.0

Table 15: Sensitivity of PDMS to the TTC weight w_{TTC} (fixed $w_{\text{EP}} = 10.0$, $w_{\text{C}} = 2.0$).

w_{TTC}	NC	DAC	TTC	Conf.	EP	PDMS
5.0	97.9	97.3	94.9	100	87.3	90.8
10.0	98.5	97.7	95.9	100	85.1	90.5
20.0	98.6	97.7	96.2	100	84.5	90.5
30.0	98.5	97.8	96.1	100	84.5	90.4

lacks sufficient diversity to demonstrate the benefits of high-level command and CoT reasoning, so we keep these guidance optional.

Impact of Different Discount Factors. Tab. 12 shows the impact of the discount factor γ on RL fine-tuning. When $\gamma = 1.0$, all timesteps, including the very noisy early steps, contribute equally to the policy gradient, which amplifies high variability noise and destabilizes learning. In contrast, setting $\gamma = 0.6$ focuses the update on later, more reliable steps and achieves the best PDMS of 90.8.

Open-loop evaluation on nuScenes. We report planning results on the nuScenes val set in Tab. 13. Trained on Bench2Drive, our method achieves strong zero-shot performance on nuScenes, and fine-tuning further yields excellent results. In particular, fine tuning substantially lowers collision rates, outperforming several prior planners, while maintaining competitive L2 displacement errors across all horizons.

PDM Score Coefficient Sensitivity Analysis. Our PDMS reward is constructed from five components: EP, TTC, Comfort (C), NC, and DAC. Concretely, the PDMS is computed as:

$$\text{PDMS} = \text{NC} \times \text{DAC} \times \left(\frac{w_{\text{EP}} \cdot \text{EP} + w_{\text{TTC}} \cdot \text{TTC} + w_{\text{C}} \cdot \text{C}}{w_{\text{EP}} + w_{\text{TTC}} + w_{\text{C}}} \right). \tag{13}$$

Tabs. 14 and 15 present the sensitivity of PDMS to the coefficients w_{EP} and w_{TTC} respectively. Increasing the EP weight w_{EP} makes the policy more aggressive, meaning that EP rises while NC, DAC, and TTC decrease slightly, and the overall PDMS correspondingly decreases when is set too large. In contrast, increasing the TTC weight w_{TTC} results in safer time-to-collision behavior with higher TTC but reduced EP, which leads to diminishing PDMS improvements as w_{TTC} increases. Based on these results, we choose the configuration $w_{\text{EP}} = 10.0$, $w_{\text{TTC}} = 5.0$, and $w_{\text{C}} = 2.0$ as our PDMS reward setting, since it provides the best trade-off between progress and safety.

D TRAINING DATASETS CONSTRUCTION

D.1 DATA COLLECTION

We collect 12 open-source driving QA datasets, including Talk2Car (Deruyttere et al., 2019), SUTD (Xu et al., 2021), NuScenes-QA (Qian et al., 2024), OmniDrive (Wang et al., 2024b), and others, yielding over 3.1 million question-answer pairs that cover perception, prediction, and planning tasks across diverse real-world scenarios.

Talk2car (Deruyttere et al., 2019) is built on the nuScenes (Caesar et al., 2020) dataset and contains 850 videos from the nuScenes (Caesar et al., 2020) training set. This dataset has 11,959 natural language commands.

SUTD (Xu et al., 2021) contains 10,080 in-the-wild videos and annotated 62,535 QA pairs. These videos are obtained through a combination of online collection and offline shooting, covering various weather conditions, times, and road conditions.

DRAMA (Malla et al., 2023) is a dataset collected to investigate risk location and natural language description in driving scenarios. It contains 17,785 interactive driving scenarios.

NuScenes-QA (Qian et al., 2024) encompasses 34,149 complex autonomous driving scenes and 459,941 question-answer pairs, with various types of questions. It aims to evaluate a model's ability to understand and reason about complex visual data in multi-modal, multi-frame, and outdoor scenarios.

DriveGPT4 (Xu et al., 2024) is built based on the BDD-X (Kim et al., 2018) dataset, which contains about 20,000 samples. By dividing them into 16,803 training segments and 2,123 testing segments, question-answer pairs are generated using the control signal data and text annotations.

LingoQA (Marcu et al., 2024) contains 28K unique short video scenarios and 419K annotations. The dataset covers various questions related to driving scenarios, including aspects such as behaviors, scenery, and perception.

DriveLM (Sima et al., 2024) consists of a training set of 4,072 frames and a validation set of 799 frames, with an average of 91.4 QA pairs per frame.

MAPLM (Cao et al., 2024) contains point-cloud BEV projections and surround view images of various traffic scenes, such as highways and urban roads, and is equipped with element-level, lane-level, and road-level scene descriptions.

NuInstruct (Ding et al., 2024) is a dataset constructed based on Nuscenes (Caesar et al., 2020), containing 91K multi-view video instruction-response pairs in 17 subtasks.

CODA-LM (Chen et al., 2024a) comprises 9,768 real-world driving scenarios with 41,722 textual annotations for critical road entities and 21,537 annotations for road corner cases.

OminiDrive (Wang et al., 2024b) covers 3D perception, reasoning, and planning tasks, including offline and online question-response tasks.

Senna (Jiang et al., 2024a) design a series of planning-oriented QAs including scene description, traffic signal detection, vulnerable road user identification, motion intention prediction, meta-action planning and planning explanation. Since the senna dataset is not publicly available, we used Qwen2.5-VL-72B (Bai et al., 2025) for question-answer data annotation.

D.2 SCALABLE HIERARCHICAL DATA PIPELINE

To systematically enhance VLM performance for autonomous driving, we design a scalable hierarchical data pipeline consisting of three stages: *Generation*, *Refinement*, and *Quality Control*, as shown in Fig. 2. This design allows us to construct diverse, semantically consistent, and high-quality annotations at scale.

Generation. We first leverage Qwen2.5-VL (Bai et al., 2025) with crafted prompts to generate annotations across the full spectrum of autonomous driving tasks on NAVSIM (Dauner et al., 2025). These tasks span perception (e.g., scene description, key object identification, road marking recognition, traffic light classification, vulnerable road user detection), prediction (e.g., motion prediction), planning (e.g., high-level command prediction and decision explanation), and advanced reasoning (e.g.,

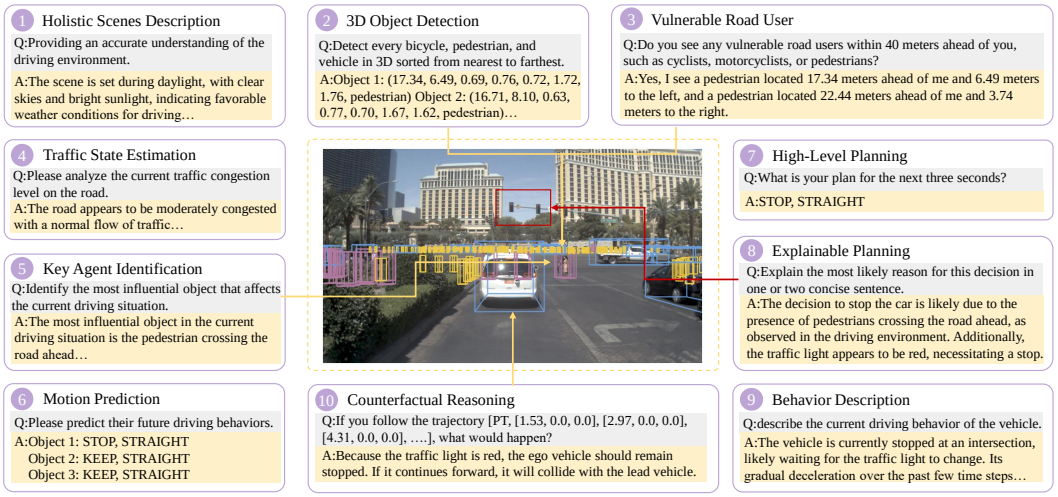

Figure 7: **Example of data generated by our Scalable Hierarchical Data Pipeline.** The pipeline produces structured QA annotations that cover four levels of autonomous-driving capability, from *Foundational Perception* and *Dynamic Understanding* to *Planning and Reasoning* and *Advanced Reasoning*, as illustrated by the multi-task QA set in this scene.

counterfactual scenarios inspired by OmniDrive (Wang et al., 2024b)). To strengthen supervision, we further incorporate NAVSIM's existing sensor and trajectory labels into the generation process. Applying this stage yields a large pool of candidate QA pairs.

Refinement. Since open-source datasets employ heterogeneous formats, we unify them through normalization and linguistic enrichment. (i) *Data Normalization:* Different datasets adopt different bounding-box styles. For example, DriveLM (Sima et al., 2024) represents an object as "<c2,CAM_BACK,864.2,468.3>", while NuInstruct (Ding et al., 2024) uses "<car>[c2,584,478,603,516]". We convert all such variants into a standardized tag format: "<car><FRONT_VIEW><box>[x_1, y_1, x_2, y_2]</box>" following the InternVL3 (Zhu et al., 2025) pre-training convention. Coordinates x_1, y_1, x_2, y_2 are rescaled to the integer range [0,1000] relative to image resolution. (ii) *Data Augmentation:* To enrich linguistic diversity, especially for datasets with limited QA templates (e.g., CODA-LM with only three formats, DRAMA with terse answers), we employ a two-step process. First, an LLM paraphrases question templates to expand structural variation. Second, Qwen2.5-VL is prompted with the original image, question, and answer to generate more detailed, natural responses. This refinement ensures consistency in structure and greater variety in language.

Quality Control. Finally, we implement a rigorous filtering step. Qwen2.5-VL assigns each QA pair a quality score based on predefined linguistic and semantic criteria. Any pair scoring below 60 is discarded. After this filtering process, we retain 2.3M high-quality QA pairs. Notably, applying the pipeline to NAVSIM produces 752K well-structured pairs, which we use to fine-tune the VLM, substantially enhancing its planning and reasoning capabilities.

D.3 Dataset Statistics

The dataset consists of 41% perception samples, 11% prediction samples, and 24% planning samples, aimed at improving VLMs' understanding of driving scenarios. We also include 24% visual instruction samples to maintain the model's instruction-following ability. For NAVSIM training, ReCogDrive is trained using a mixture of NAVSIM trajectory data (5%), our newly generated 752K cognition–aligned QA pairs (22.9%), open–source driving QA datasets totaling 2.3M samples (68.1%), and 665K LLaVA instruction data (3.9%). This composition balances driving–specific reasoning with general VLM instruction capability. For Bench2Drive adaptation, the NAVSIM–trained model is further fine–tuned on Bench2Drive execution trajectories (79.2%) together with Bench2Drive driving–QA annotations (20.8%), enabling the model to acquire simulation–specific driving priors required for closed–loop CARLA evaluation.

E EXPERIMENT DETAILS

In this section, we first introduce the evaluation metrics of NAVSIM and Bench2Drive, and then detail our model configuration, the hyperparameters used in the three-stage training and evaluation, and our hardware setup.

Evaluation Metrics. We evaluate our method on two primary benchmarks. For the planning-oriented NAVSIM benchmark, we use the official Predictive Driver Model Score (PDMS), a closed-loop metric that holistically assesses safety (NC, DAC, TTC), comfort (C), and progress (EP):

$$\text{PDMS} = \text{NC} \times \text{DAC} \times \left(\frac{5 \cdot \text{EP} + 5 \cdot \text{TTC} + 2 \cdot \text{C}}{12} \right). \tag{14}$$

For the CARLA-based Bench2Drive benchmark, which focuses on safety-critical scenarios, we report the Success Rate (SR) and the average Driving Score (DS). The DS combines Route Completion (RC) with multiplicative penalties for infractions (IS):

$$\text{SR} = \frac{N_{\text{success}}}{N_{\text{total}}}; \quad \text{DS} = \frac{1}{N_{\text{total}}} \sum_{i=1}^{N_{\text{total}}} \left(\text{RC}_i \times \prod_j \text{IS}_{i,j} \right). \tag{15}$$

Model Architecture and Hyperparameter Details. Our model architecture consists of two main components: Vision-Language Models (VLMs) and a diffusion-based trajectory planner. For the Vision-Language Models, we utilize the pre-trained InternVL3-8B and InternVL3-2B (Zhu et al., 2025) model. The model processes visual inputs by splitting images into patches: on NAVSIM, we use a single front-view image divided into 9 patches, while on Bench2Drive we use multi-view inputs from six cameras, each cropped into 3 patches. The input images are cropped into 448x448 pixel patches. For the diffusion planner, we use the DiT (Peebles & Xie, 2023) architecture, employing DDPM/DDIM (Ho et al., 2020) denoising methods. During training, the denoising process involves 100 steps, while for inference, the diffusion process is reduced to 5 steps. The hidden layer size of the DiT architecture is set to 384, with a head size of 8 and 16 layers.

Table 16: **Hyperparameters for ReCogDrive.**

Stage	Parameter	Value
I	Number of epochs	3
	Batch size	1024
	Learning rate	$4e^{-5}$
	Weight decay	0.05
	Warmup ratio	0.10
	Learning rate schedule	Cosine
II	Number of epochs	200
	Batch size	512
	Learning rate	$1e^{-4}$
	Learning rate schedule	Cosine
	Weight decay	1×10^{-4}
III	Number of epochs	10
	Batch size	128
	Learning rate	$1e^{-4}$
	Learning rate schedule	Cosine
	BC loss weight	$1e^{-2}$
	Denoised clip threshold	± 1.0
	Noise clip threshold	± 3.0
	Minimum denoising std	0.02
	Minimum log-variance std	0.10
	Discount factor	0.6

Training Configuration. In the first stage, we fine-tune the InternVL3 VLM for three epochs with all parameters unfrozen and a batch size of 1,024 on a curated 3M real-world driving QA corpus

that unifies Talk2Car (Deruyttere et al., 2019), SUTD (Xu et al., 2021), DRAMA (Malla et al., 2023), NuScenes-QA (Qian et al., 2024), DriveGPT4 (Xu et al., 2024), LingoQA (Marcu et al., 2024), DriveLM (Sima et al., 2024), MAPLM (Cao et al., 2024), NuInstruct (Ding et al., 2024), CODA-LM (Chen et al., 2024a), OmniDrive (Wang et al., 2024b), Senna (Jiang et al., 2024a), LLaVA Instruction-QA (Liu et al., 2023a) and 752K additional QA pairs generated by our hierarchical data pipeline, providing a strong real-world foundation tailored for both DriveBench and NAVSIM. We use AdamW with a base learning rate of $4e^{-5}$, weight decay of 0.05, and a cosine learning rate schedule with a 10% linear warmup. For CARLA-based simulation, we further adapt the real-world–trained model by fine-tuning it with Bench2Drive trajectory data and Bench2Drive-QA using identical hyperparameters to ensure compatibility with the CARLA environment.

In the second stage, we train the diffusion-based planner with imitation learning on trajectory supervision from both NAVSIM and Bench2Drive for 200 epochs and a batch size of 512, using AdamW with a learning rate that warms up to $1e^{-4}$ over the first 1.5% of steps, then decays cosinely to $1e^{-6}$, and a weight decay of $1e^{-4}$.

In the third stage, we perform DiffGRPO reinforcement learning using the full NAVSIM and Bench2Drive training data for 10 epochs with a batch size of 128, using AdamW and a cosine schedule that decays the learning rate from $1e^{-4}$ to 0. Additionally, we stabilize diffusion training and inference by clipping the reconstructed clean estimate x_0 to ± 1.0, clipping Gaussian noise samples to ± 5.0, enforcing a nonzero floor on the denoising standard deviation σ_t of 0.02 for training, clamping σ_t to at least 0.10 when computing $\log p(x_{t-1} \mid x_t)$, and applying a discount factor $\gamma = 0.6$ during RL fine-tuning to downweight early, noisy timesteps. During RL fine-tuning, we optimize the planner using the PDMS reward with weighting coefficients $\alpha = 10.0$ (EP), $\beta = 5.0$ (TTC), and $\gamma = 2.0$ (Comfort), which we identified as providing the best trade-off between progress and safety.

Hardware Configuration. We implement ReCogDrive on Debian with PyTorch, training across four nodes—each equipped with an Intel® Xeon® Platinum 8457C CPU and eight NVIDIA H20 GPUs (32 GPUs in total). Inference is performed on a single node with 8 GPUs.

F Limitations

Although ReCogDrive achieves state of the art performance on the NAVSIM benchmark, it still faces several limitations. These include the difficulty of processing multiple camera inputs, handling video frame sequences, and relatively high inference latency. Future work may address these issues by designing a 3D vision encoder that aligns with textual features and developing more efficient model architectures. We also plan to deploy and evaluate our model on real vehicles.

G LLM Usage Statement

Large Language Models (LLMs) were employed solely as writing assistants to improve the clarity, grammar, and readability of the manuscript. They were not involved in research ideation, methodology design, data analysis, or result interpretation.

H Broader Impacts

Our research promotes the application of Vision-Language Models (VLMs) in the autonomous driving domain. Through simulator-assisted reinforcement learning, our model more effectively mitigates collision risk and generalizes to rare, challenging scenarios. This advancement could lead to safer, more reliable autonomous systems capable of handling real-world driving scenarios.

I Qualitative Results

We first present extensive qualitative visualizations of ReCogDrive on NAVSIM and Bench2Drive, highlighting its ability to produce safe and smooth trajectories. Next, we provide trajectory comparisons between ReCogDrive-IL and ReCogDrive-RL to demonstrate the effectiveness of our proposed DiffGRPO. We further showcase dialogue examples generated by ReCogDrive, illustrating its cog-

nitive reasoning capability. Finally, we analyze representative failure cases on NAVSIM to provide insights into current limitations.

I.1 Qualitative Results on Navtest Splits

We present representative cases from the Navtest splits, highlighting ReCogDrive's ability to follow navigation instructions while ensuring safety and smoothness (see Fig. 8 and Fig. 11).

I.2 Qualitative Results on Bench2Drive Test Scenarios

We evaluate ReCogDrive on challenging scenarios from Bench2Drive, demonstrating its robustness under diverse traffic conditions and rare corner cases, while consistently maintaining strong performance in closed-loop settings.

I.3 Comparison Before and After Reinforcement Learning

Representative qualitative comparisons are shown in Fig. 12–16, where we contrast Transfuser, imitation learning (IL), and reinforcement learning (RL) variants of ReCogDrive, demonstrating the progressive improvements in decision making, trajectory stability, and safety awareness.

I.4 Failure Cases

We also present representative failure cases of ReCogDrive on the Navsim benchmark, as shown in Fig. 17. These include instances of aggressive driving caused by the model's tendency to prioritize ego progress, leading to assertive maneuvers. In addition, the relatively weak perception capability of current VLMs means that directly feeding multi-view camera inputs sometimes results in suboptimal performance, particularly in turning scenarios. We also observe unsafe following distances due to insufficient modeling of surrounding vehicle behaviors, reflecting the limitations of VLMs in motion prediction. Finally, we identify cases where predicted trajectories are visually close to the ground truth but still scored as failures, suggesting that the evaluation metrics may suffer from false negatives.

I.5 Model–Human Dialogue

As shown in Fig. 18–20, ReCogDrive engages in interactive dialogue by providing detailed scene descriptions, recognizing traffic signs, reasoning about driving intent, and generating safe turning trajectories.

Figure 8: Qualitative results on the Navtest benchmark.

Figure 9: Qualitative results on the Navtest benchmark.

(a) Turning Right

(b) Turning Left

Figure 10: Qualitative results on the Bench2drive benchmark.

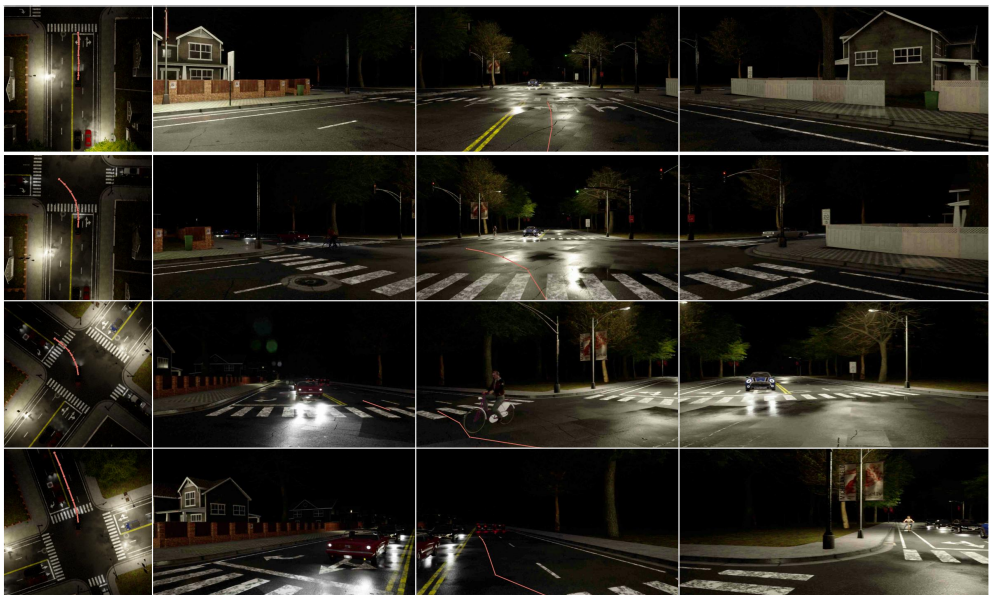

(c) Turning Left At Night

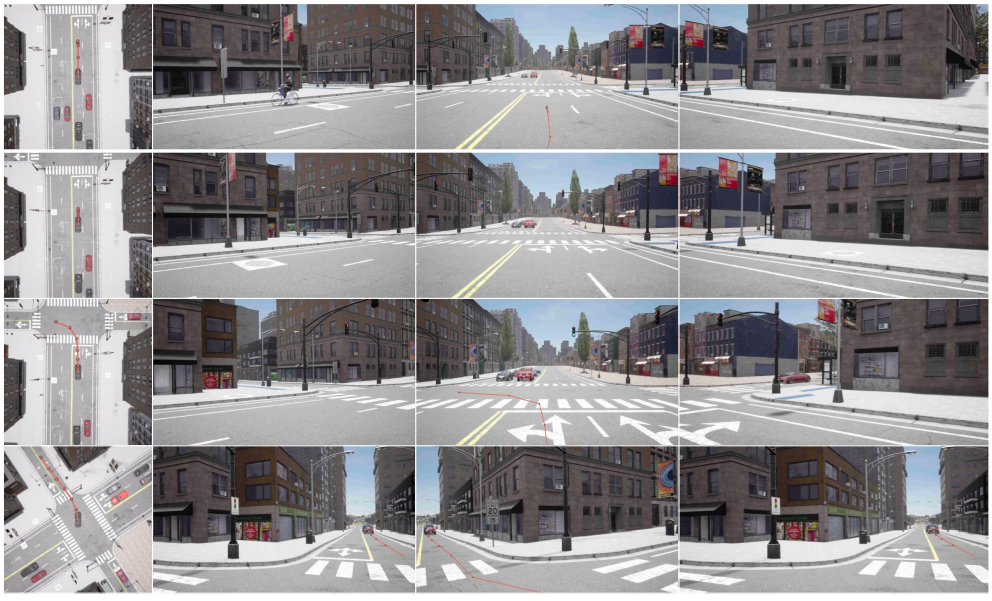

(d) Stop On Red, Proceed On Green.

Figure 11: Qualitative results on the Bench2drive benchmark.

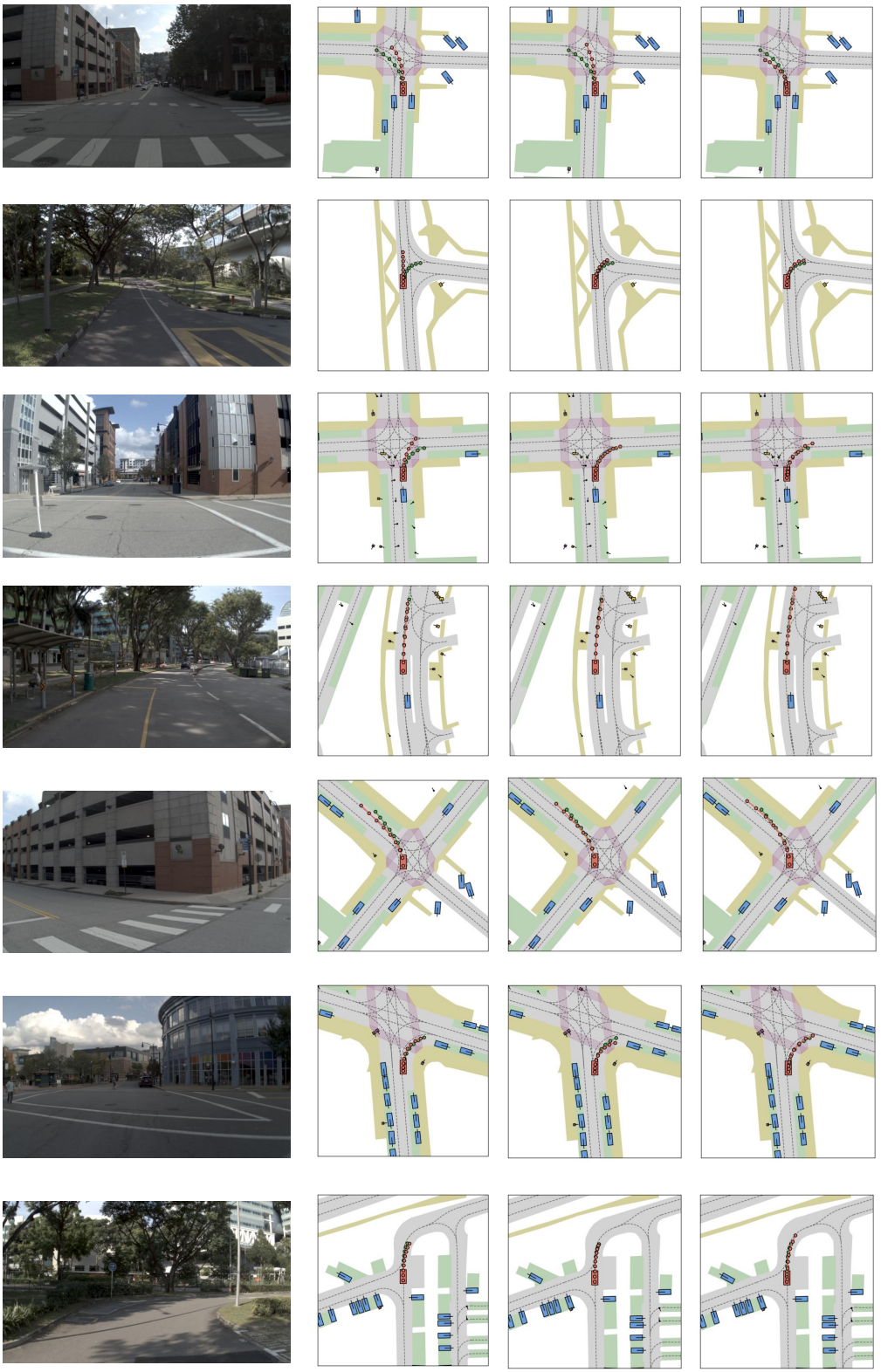

Figure 12: Qualitative comparisons on the Navtest benchmark.

Figure 13: Qualitative comparisons on the Navtest benchmark.

Figure 14: Qualitative comparisons on the Navtest benchmark.

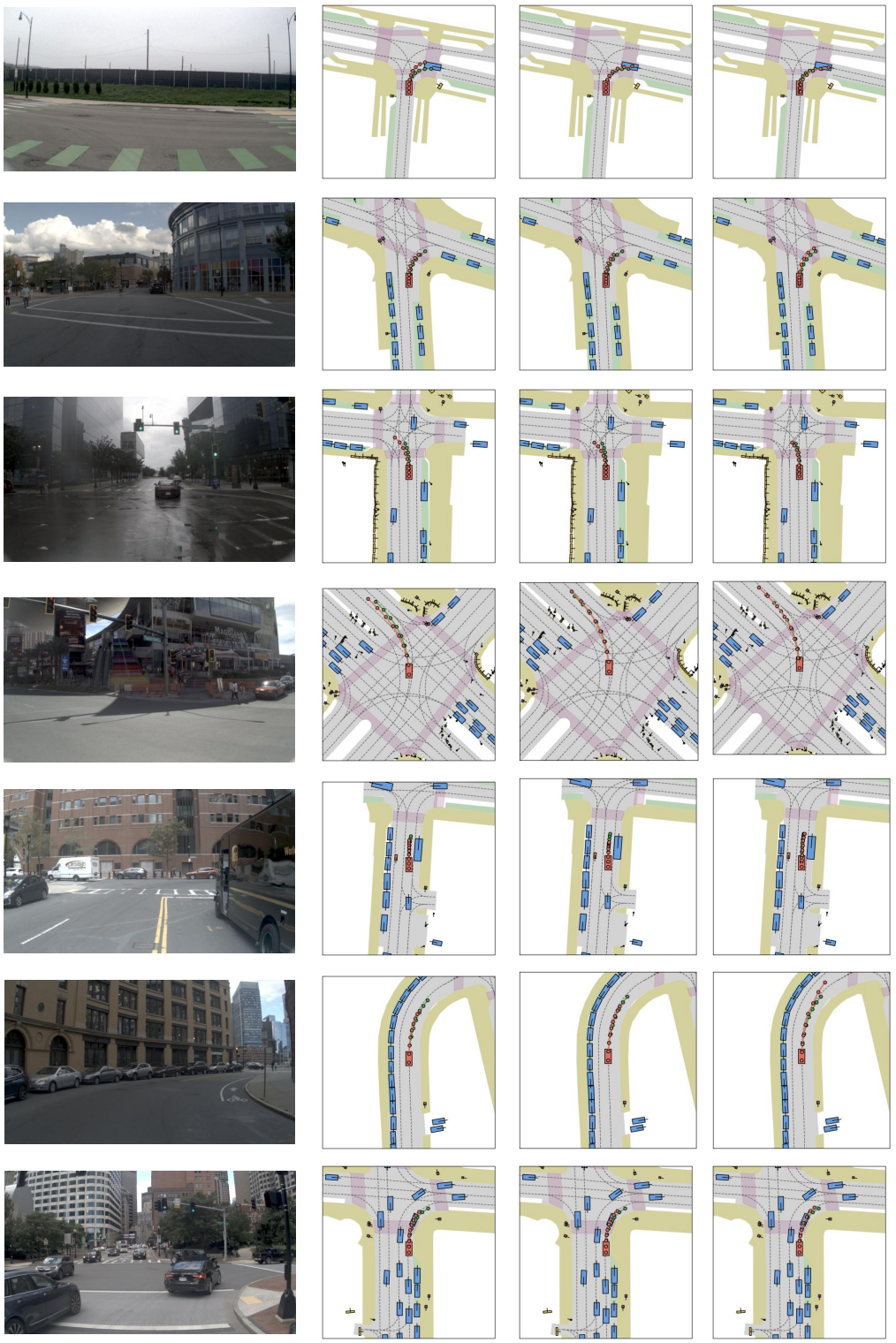

Figure 15: Qualitative comparisons on the Navtest benchmark.

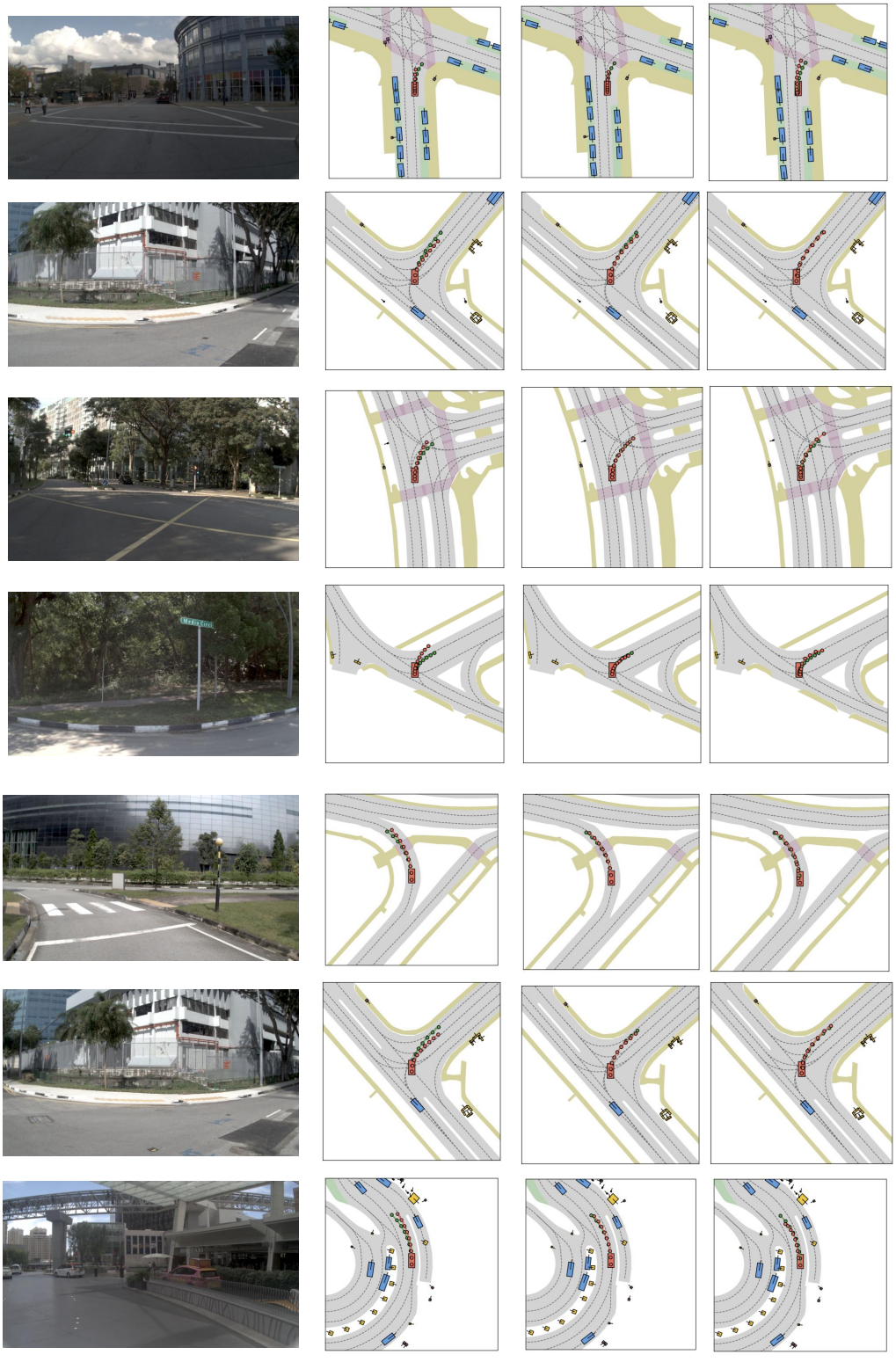

Figure 16: Qualitative comparisons on the Navtest benchmark.

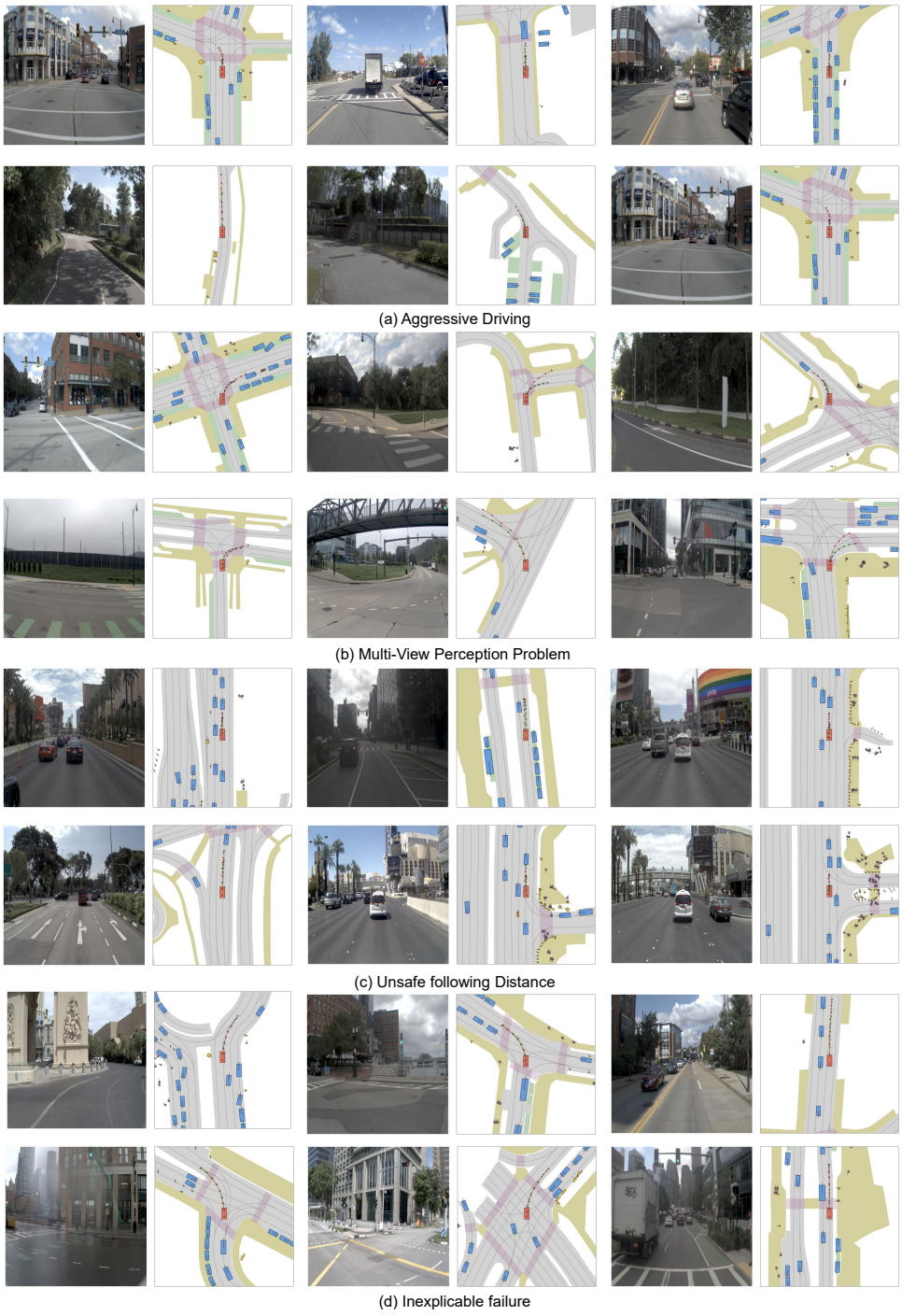

Figure 17: Representative failure cases of ReCogDrive on the Navsim benchmark, including aggressive driving, multi-view perception problem, unsafe following distances, and inexplicable failures. Zoom in for better view.

Please make a description for the driving scene.

The scene is set during daylight under a clear sky and scattered clouds. The road is smooth and appears to be a multi-lane highway with no visible obstacles. Traffic lights ahead are showing green, allowing for continued forward movement. A silver sedan is positioned in front on the right lane, moving steadily ahead, while a white van is further up, also proceeding forward. On the far right, a black car is visible, maintaining its lane. A truck is observed slightly ahead on the left, and a bus is further back, both maintaining their lanes and moving forward.

Identify and describe the road markings and signs.

The image shows displays a clear road scene where white dashed lines indicate lane separations, guiding drivers to stay within their respective lanes, while a white arrow on the road suggests the direction of travel for the lane it's in. A round blue sign with a red slash over a black right-turning arrow signals that right turns are prohibited at the junction ahead, requiring drivers to either proceed straight or turn left if permitted. The presence of a pedestrian crossing is implied by the zebra lines on the left, advising drivers to be cautious and ready to stop if pedestrians are present.

Predict the vehicle's trajectory based on the front-view image, historical trajectory and command.

Figure 18: An example shows ReCogDrive's capability in road sign recognition and intersection-turn planning: given a front-view image and a user query, ReCogDrive generates a detailed scene description, identifies key traffic signs at the junction, and predicts a safe turning trajectory.

Please make a description for the driving scene.

The current driving scene is set during daylight hours under partly cloudy skies, providing ample natural lighting. The road surface appears smooth and clear of any obstacles, with a few vehicles ahead maintaining a steady pace. To the left, there's a line of cars, including a dark sedan and a white sedan approaching an intersection. To the right, a taxi is visible. Caution is advised as the cars ahead are preparing to move through the intersection. The presence of well-maintained roadside greenery and the archway adds to the urban aesthetic but does not impact the driving conditions.

Identify the most influential object that affects the current driving situation.

The most influential object in the current driving situation is the traffic light ahead, which is currently red. This traffic light is crucial as it dictates the flow of vehicles and ensures safety at the intersection. The cars ahead, including a silver vehicle directly in front of the viewer, have come to a stop, indicating compliance with the traffic signal. Given the red light, the appropriate driving action is to safely come to a complete stop behind the silver vehicle, maintaining a safe following distance. This will allow the driver to respond appropriately when the light turns green, ensuring a smooth and safe transition through the intersection.

Predict the vehicle's trajectory based on the front-view image, historical trajectory and command.

Figure 19: An example shows ReCogDrive's capability in scenario understanding and trajectory planning: at a red-light intersection with braking vehicles ahead, ReCogDrive describes the traffic lights and road conditions, identifies both the traffic light and lead vehicles, and predicts an accurate stop trajectory.

Please make a description for the driving scene.

The scene is set during daylight with clear skies, suggesting favorable weather for driving. The road is a multi-lane highway with smooth surfaces. Traffic lights ahead are green, indicating that it's safe to proceed. Several vehicles are present, including a white car to the left and an orange convertible ahead, both moving forward at a moderate speed. Pedestrians can be seen on the sidewalks to the right. The overall setting is calm, with no immediate hazards or congestion. Based on this description, you can proceed with caution, maintaining a safe distance from the vehicles ahead.

Please predict the orange car future driving behaviors

The red car is positioned in the right lane, approaching an intersection with a green traffic light. Based on the visual context, the car will likely continue to keep its current speed and proceed straight through the intersection. This decision is supported by the clear visibility of the green light and the absence of any obstacles or pedestrians in the car's path.

What is your plan for the next three seconds?

KEEP, STRAIGHT

Predict the vehicle's trajectory based on the front-view image, historical trajectory and command.

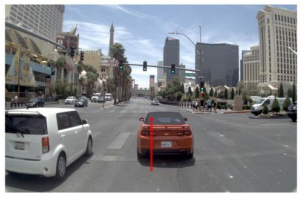

Figure 20: An example shows ReCogDrive's capability in behavior prediction and planning: at a green-light intersection, ReCogDrive describes the road and traffic conditions, identifies the green signal and the lead vehicle's behavior, generates a high-level "KEEP,STRAIGHT" command, and predicts the precise continuous trajectory for the ego vehicle.